Whole Brain Connectivity Mapping in Mouse at the Mesoscopic Scale

Partha Mitra

Cold Spring Harbor Laboratory

Jan 26, 2016

"I propose to investigate the question as to whether it is possible for machinery to show intelligent behavior." –

Intelligent Machinery (1948),
Alan Turing

MIT Technology Review

COMPUTING NEWS

3 COMMENTS

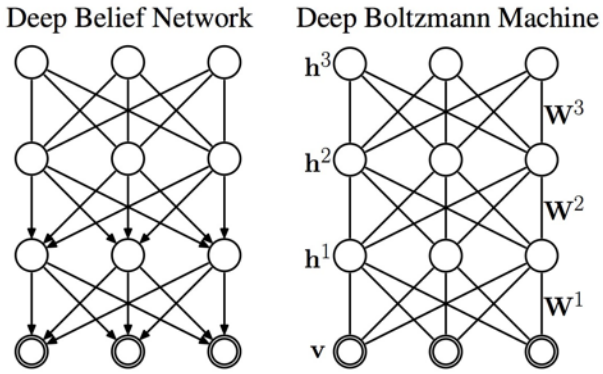

Deep Learning Catches On in New Industries, from Fashion to Finance

The machine-learning technique known as deep learning, which has shown impressive results in voice and image recognition, is finding new applications.

By Will Knight on May 31, 2015

ANNs used in "Deep Learning" algorithms are not Neurobiologically Plausible

1. Biologically implausible learning rules.
2. Require much larger training data sets than brains.
3. Have non-biological fragilities (eg dusty cars can be classified as non-cars).
4. Lack feedback and dynamics
5. Use much more power (human brain = 12W, Pentium chip ~30-100W)

Deep ANNS are essentially *Tabula Rasa* learners. Biological brains have species-specific, genetically encoded circuitry that have evolved over >10^8 years

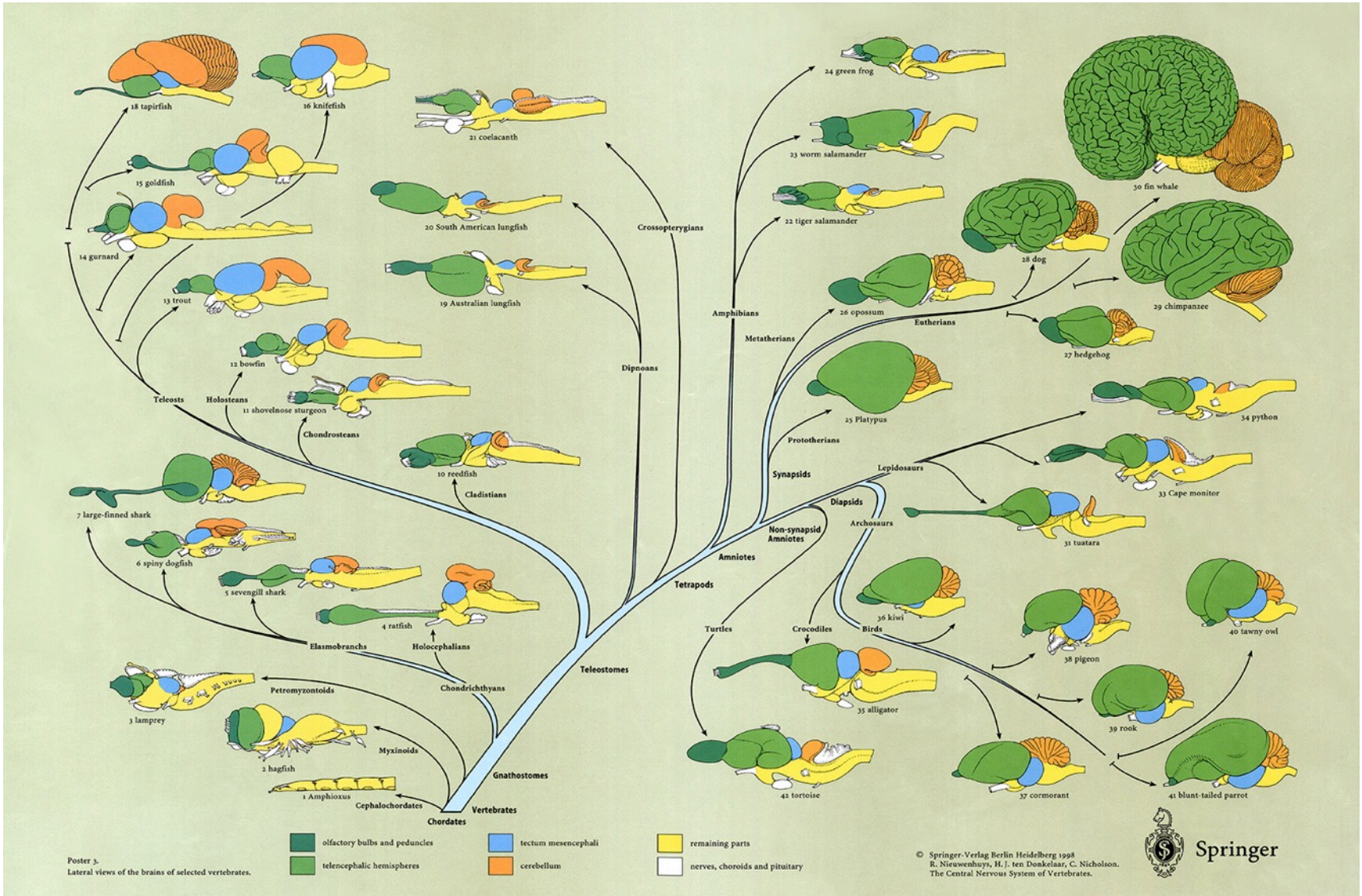

"The Grand Question, which every naturalist ought to have before him, when dissecting a whale, or classifying a mite, a fungus, or an infusorian is 'What are the laws of life' ?"

Charles Darwin, Notebook B

".. when we contemplate every complex structure and instinct as the summing up of many contrivances, each useful to the possessor, nearly the same way as when we look at any great mechanical invention as the summing up of the labor, the experience, the reason, and even the blunders of numerous workmen; when we thus view each organic being, how much more interesting, I speak from experience, will the study of natural history become!

Charles Darwin, The Origin of Species

Laws of life (intelligence etc) = Laws of design (“engineering theories”)

Engineering theories: 3C’s (communication, computation, control,
statistics a.k.a. machine learning,
in network/distributed settings)

Symmetry principles ⟷ Invariance of interface (black box models)
Universality (physics) ⟷ Universality (engineering; eg Universal Turing Model)

An example of "design"/engineering theory addressing neurobiological phenomena

Chomsky, Noam. "On certain formal properties of grammars." *Information and control* 2.2 (1959): 137-167.

Chomsky, Noam. *Knowledge of language: Its nature, origin, and use*. Greenwood Publishing Group, 1986.

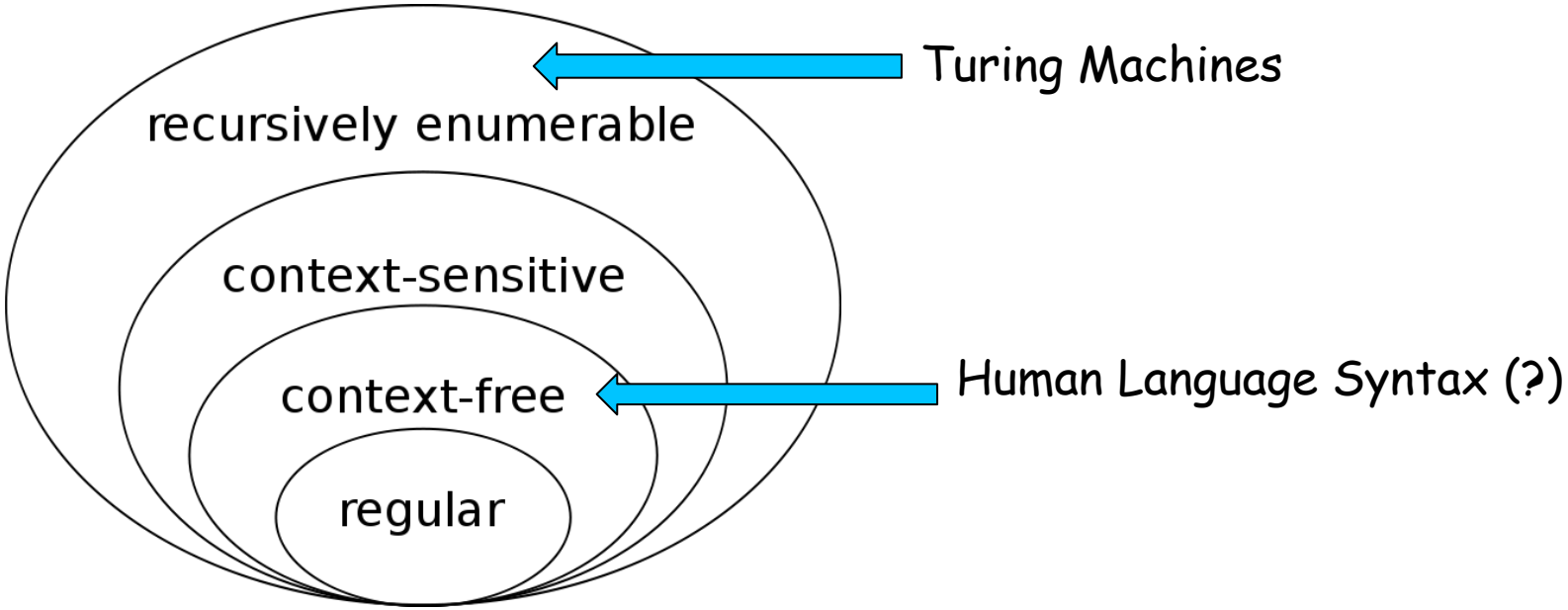

Chomsky Hierarchy of Formal Grammars (and associated automata)

We can potentially discover the principles of intelligent machines by studying real brain circuits

However after more than a century of intensive study, our knowledge of brain circuitry is still highly incomplete - hence the recent renaissance in neuroanatomical research, enabled by automation and "big data".

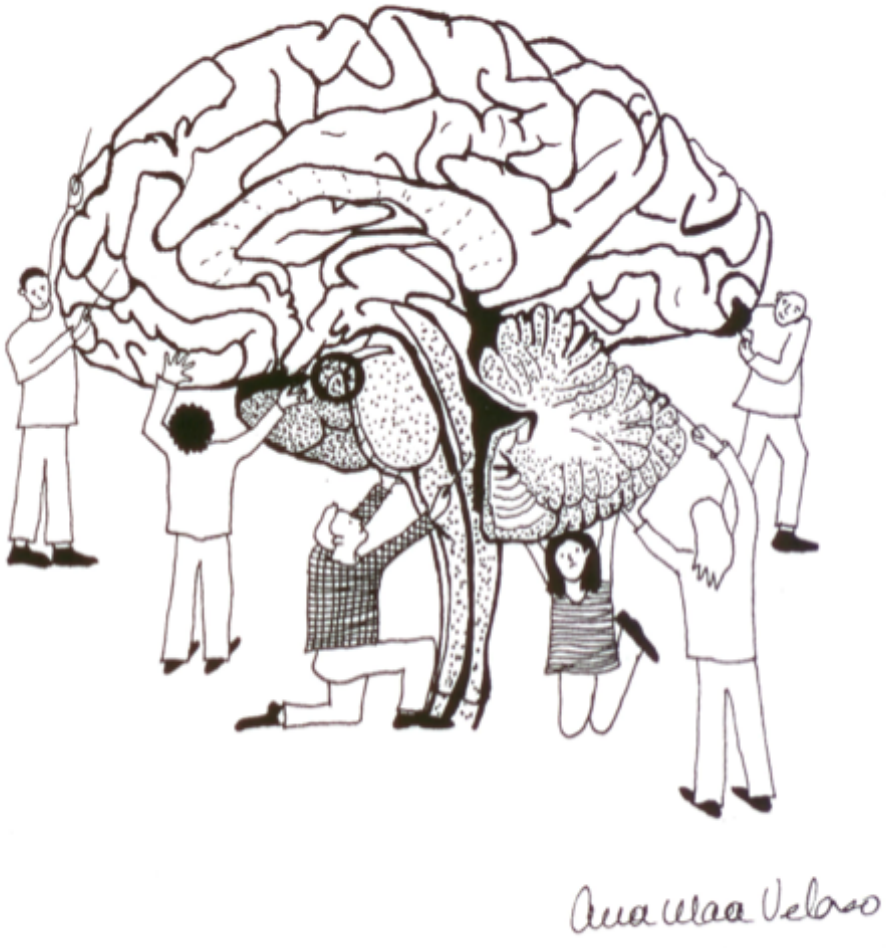

Organized a series of meetings at the Banbury Center (CSHL) (2007,2008)

Leading to a proposal for systematic brain-wide mapping of connectivity at a **mesoscopic scale** in model organisms, starting with Mouse.

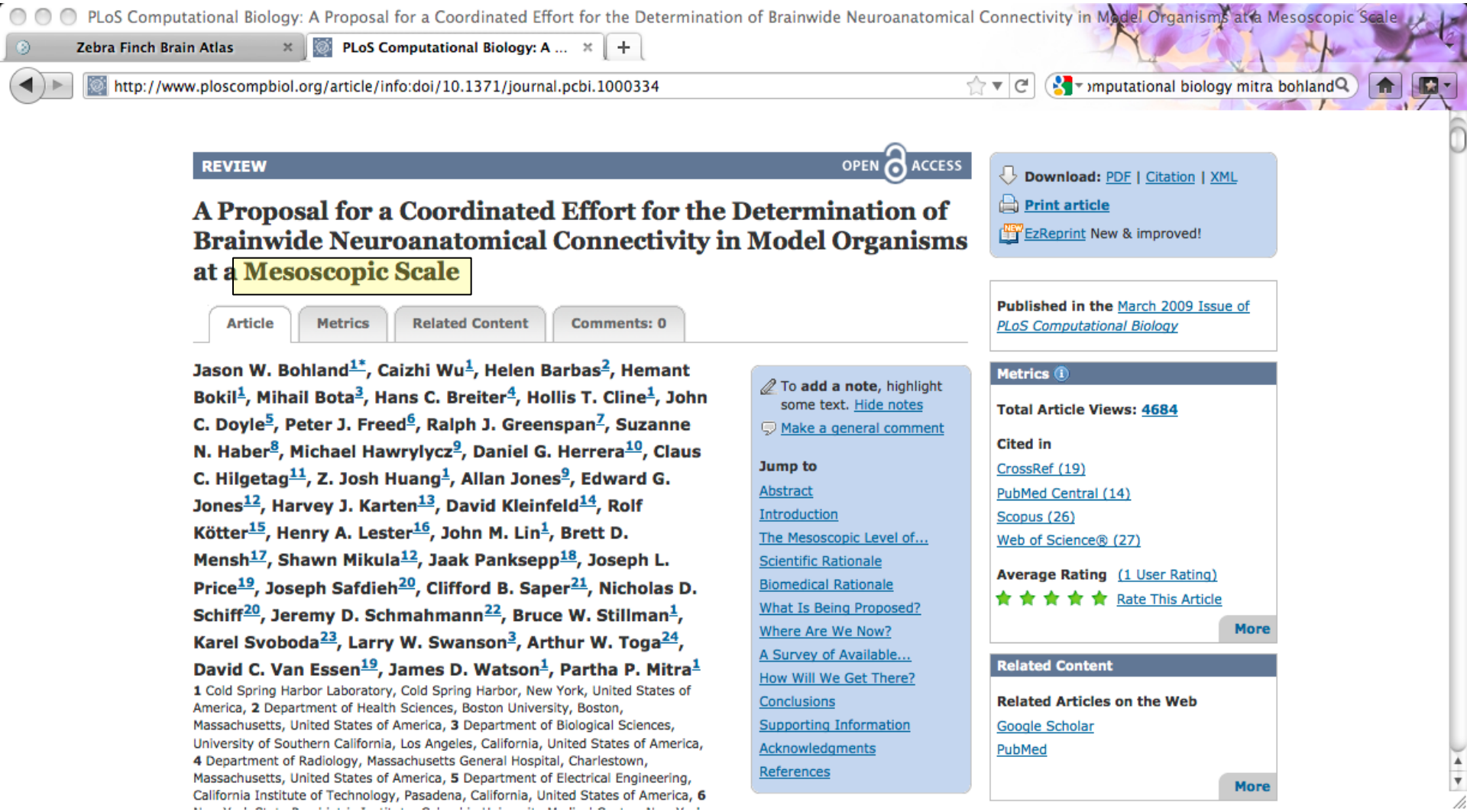

PLoS Computational Biology: A Proposal for a Coordinated Effort for the Determination of Brainwide Neuroanatomical Connectivity in Model Organisms at a Mesoscopic Scale

Zebra Finch Brain Atlas | PLoS Computational Biology: A ...

http://www.ploscompbiol.org/article/info:doi/10.1371/journal.pcbi.1000334

mputational biology mitra bohland

REVIEW OPEN ACCESS

A Proposal for a Coordinated Effort for the Determination of Brainwide Neuroanatomical Connectivity in Model Organisms at a Mesoscopic Scale

Article | Metrics | Related Content | Comments: 0

Jason W. Bohland[1*], Caizhi Wu[1], Helen Barbas[2], Hemant Bokil[1], Mihail Bota[3], Hans C. Breiter[4], Hollis T. Cline[1], John C. Doyle[5], Peter J. Freed[6], Ralph J. Greenspan[7], Suzanne N. Haber[8], Michael Hawrylycz[9], Daniel G. Herrera[10], Claus C. Hilgetag[11], Z. Josh Huang[1], Allan Jones[9], Edward G. Jones[12], Harvey J. Karten[13], David Kleinfeld[14], Rolf Kötter[15], Henry A. Lester[16], John M. Lin[1], Brett D. Mensh[17], Shawn Mikula[12], Jaak Panksepp[18], Joseph L. Price[19], Joseph Safdieh[20], Clifford B. Saper[21], Nicholas D. Schiff[20], Jeremy D. Schmahmann[22], Bruce W. Stillman[1], Karel Svoboda[23], Larry W. Swanson[3], Arthur W. Toga[24], David C. Van Essen[19], James D. Watson[1], Partha P. Mitra[1]

1 Cold Spring Harbor Laboratory, Cold Spring Harbor, New York, United States of America, **2** Department of Health Sciences, Boston University, Boston, Massachusetts, United States of America, **3** Department of Biological Sciences, University of Southern California, Los Angeles, California, United States of America, **4** Department of Radiology, Massachusetts General Hospital, Charlestown, Massachusetts, United States of America, **5** Department of Electrical Engineering, California Institute of Technology, Pasadena, California, United States of America, **6**

To add a note, highlight some text. Hide notes

Make a general comment

Jump to

Download: PDF | Citation | XML

Print article

EzReprint New & improved!

Published in the March 2009 Issue of *PLoS Computational Biology*

Metrics

Total Article Views: 4684

Cited in

CrossRef (19)
PubMed Central (14)
Scopus (26)
Web of Science® (27)

Average Rating (1 User Rating)

Rate This Article

More

Related Content

Related Articles on the Web

Google Scholar
PubMed

More

What is the Mesoscopic Scale in Neuroanatomy?

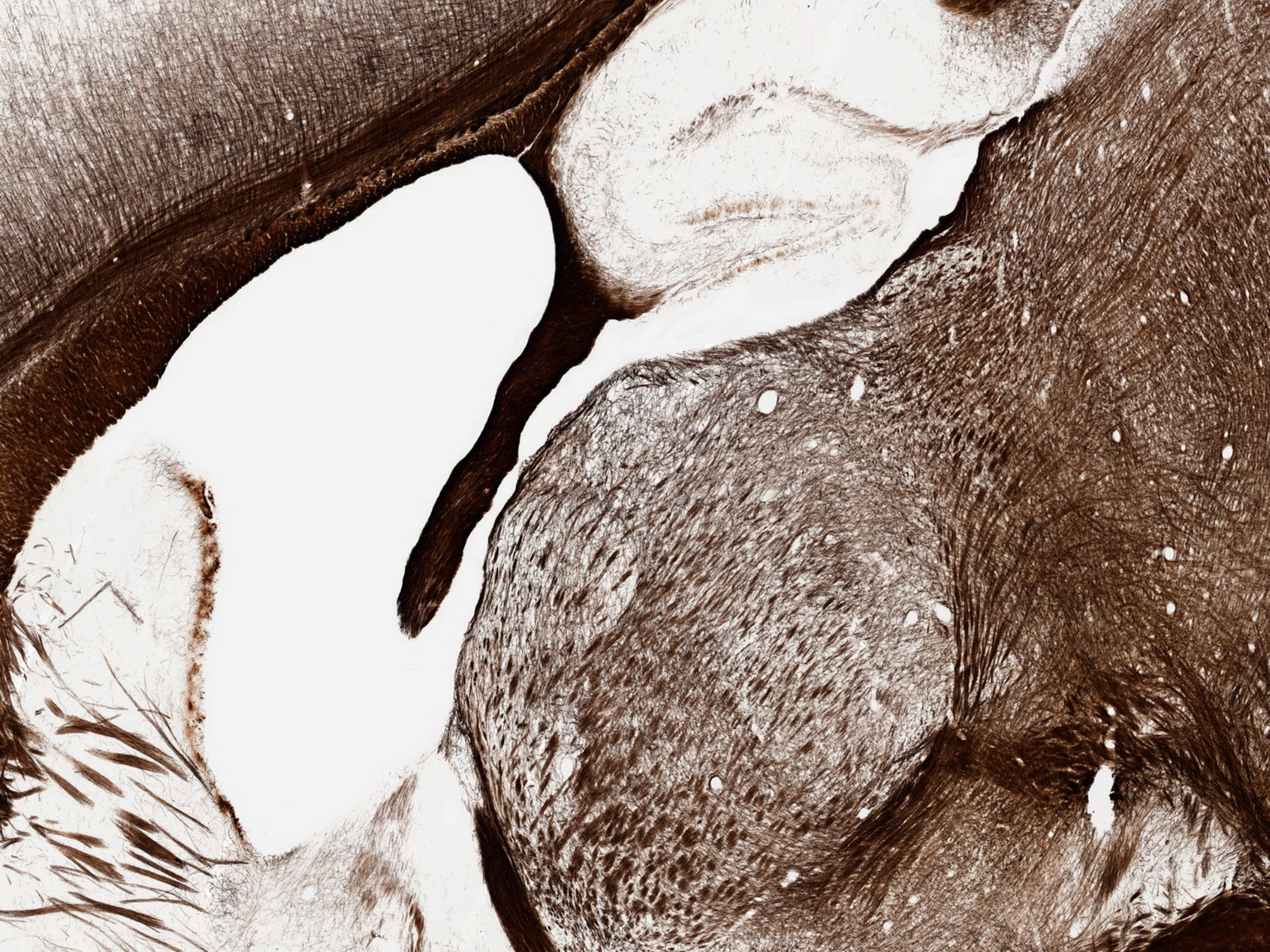

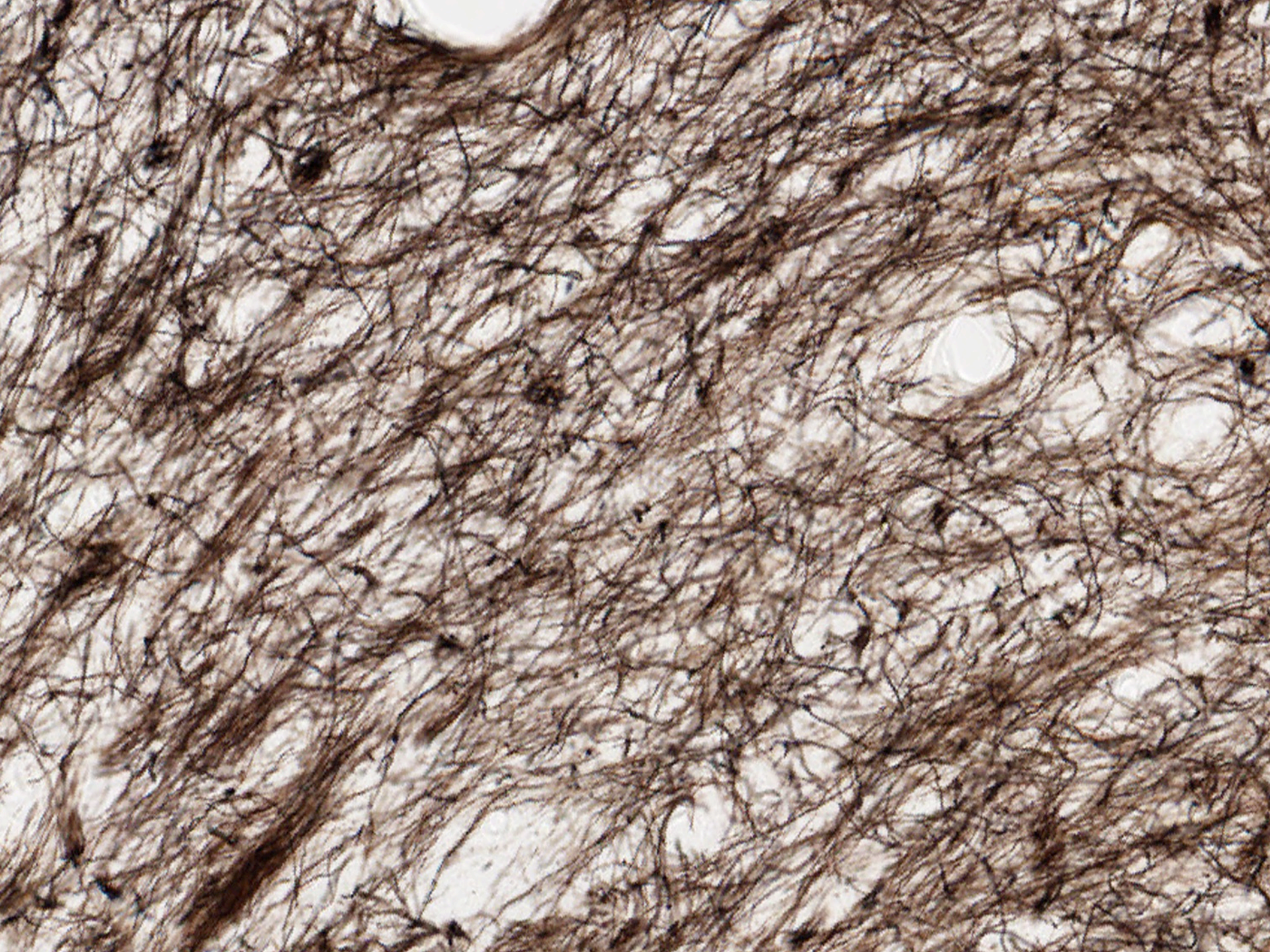

The mesoscopic scale of analysis of brain architecture may be defined as the transitional point between a microscopic scale at which individual variation is prominent and the more macroscopic level where a more stable, species-typical neural architecture is observed.

P.P.Mitra, The Circuit Architecture of Whole Brains at the Mesoscopic Scale, Neuron (2014), http://dx.doi.org/10.1016/ j.neuron.2014.08.055

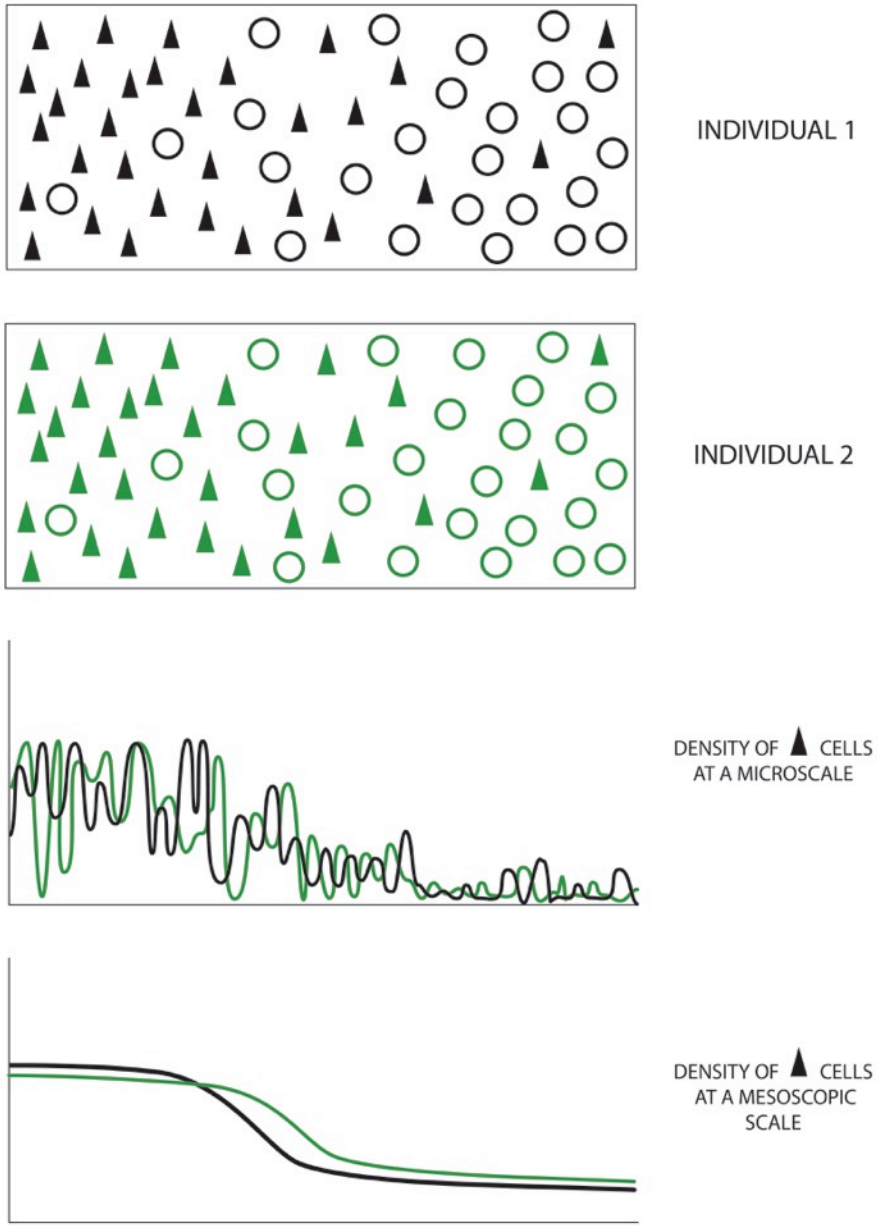

FIG. 1

Tree-Architecture of Individual Neurons

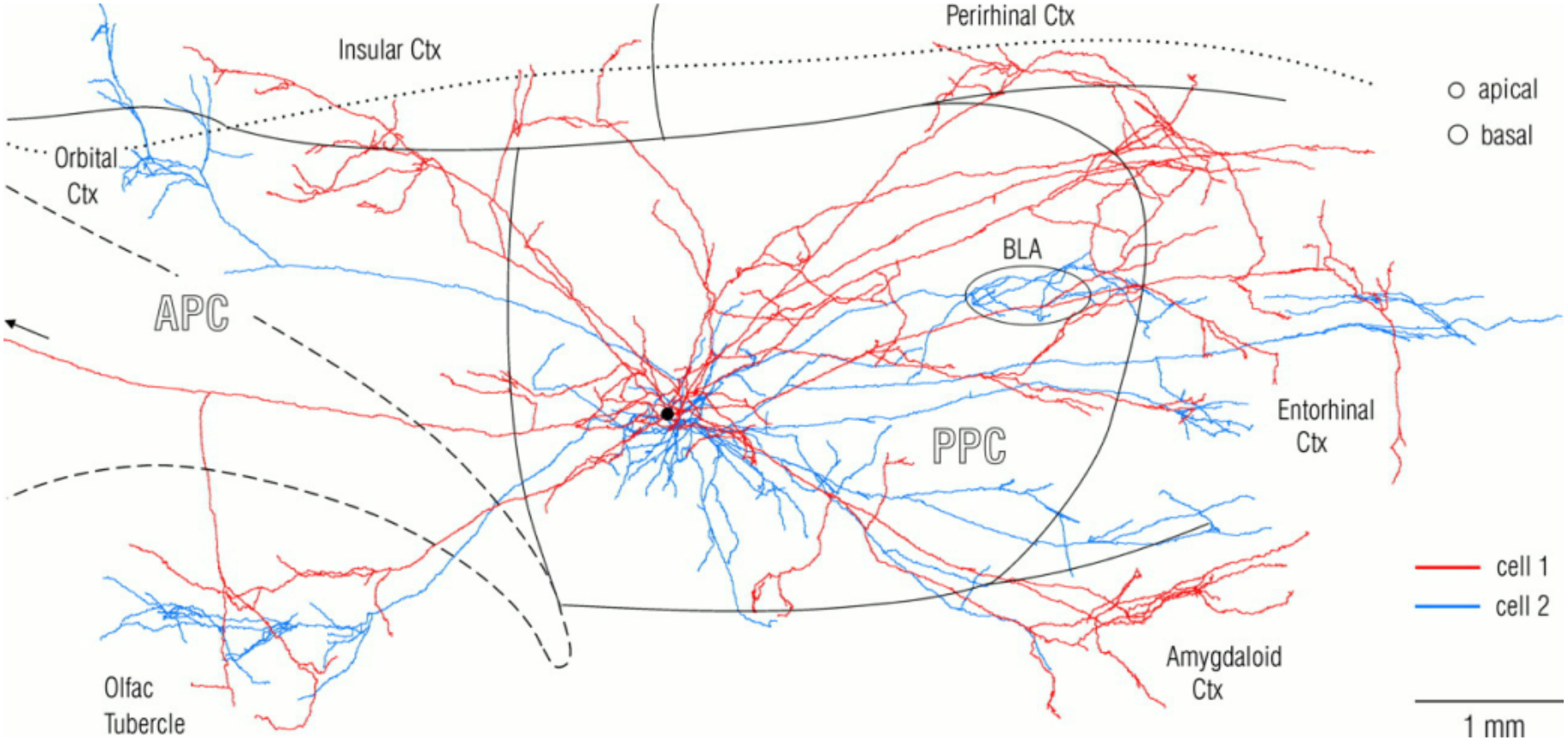

Individual Neurons can form branched trees spanning the brain
(e.g: Single Pyramidal neuron tracings, rat Piriform cortex,
J Neurosci. 2000 Sep 15;20(18):6974-82.
Johnson DM, Illig KR, Behan M, Haberly LB.)

Approach: Scaling Up Classical Neuroanatomy

Localized injections of neuronal tracer substances to label neurons

1. Anterograde tracers: "Soma -> Axon terminals"
2. Retrograde tracers: "Axon terminals -> Soma"

- Systematically apply to whole brain
- Automate, digitize, analyze.

Anterograde + Retrograde labelling allows mapping of local inputs + outputs of a region

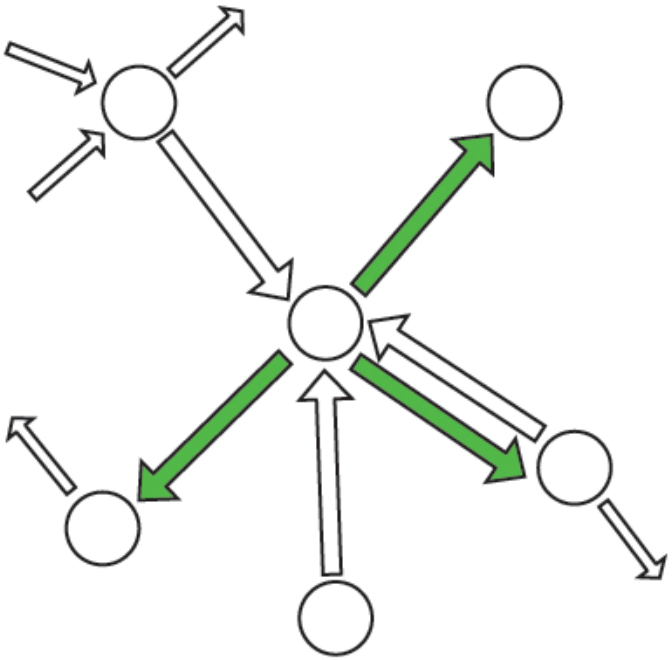

Whole Brain Reconstructions AAV injection in MOp

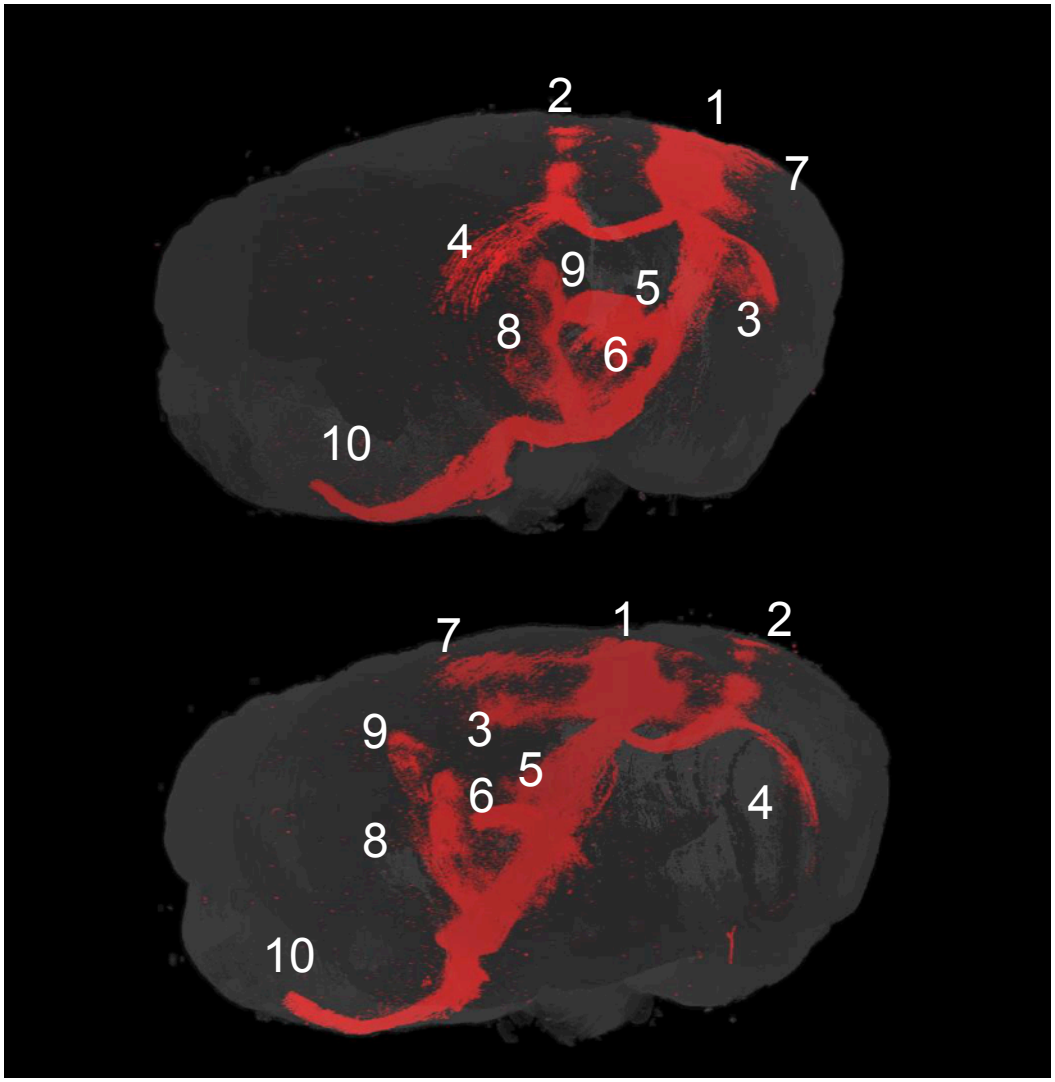

AAV injected in MOp

1. MOp, ipsi (injected)
2. MOp, contra
3. STRd, ipsi
4. CC, contra
5. GP, ipsi
6. TH, ipsi
7. SSp, ipsi
8. MB, ipsi
9. SC, ipsi
10. py, ipsi

Anterograde + Retrograde labelling allows mapping of local inputs + outputs of a region

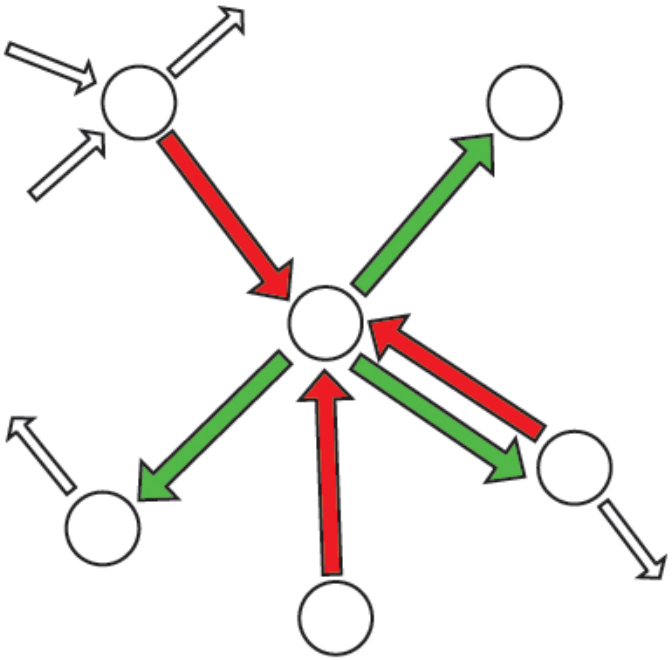

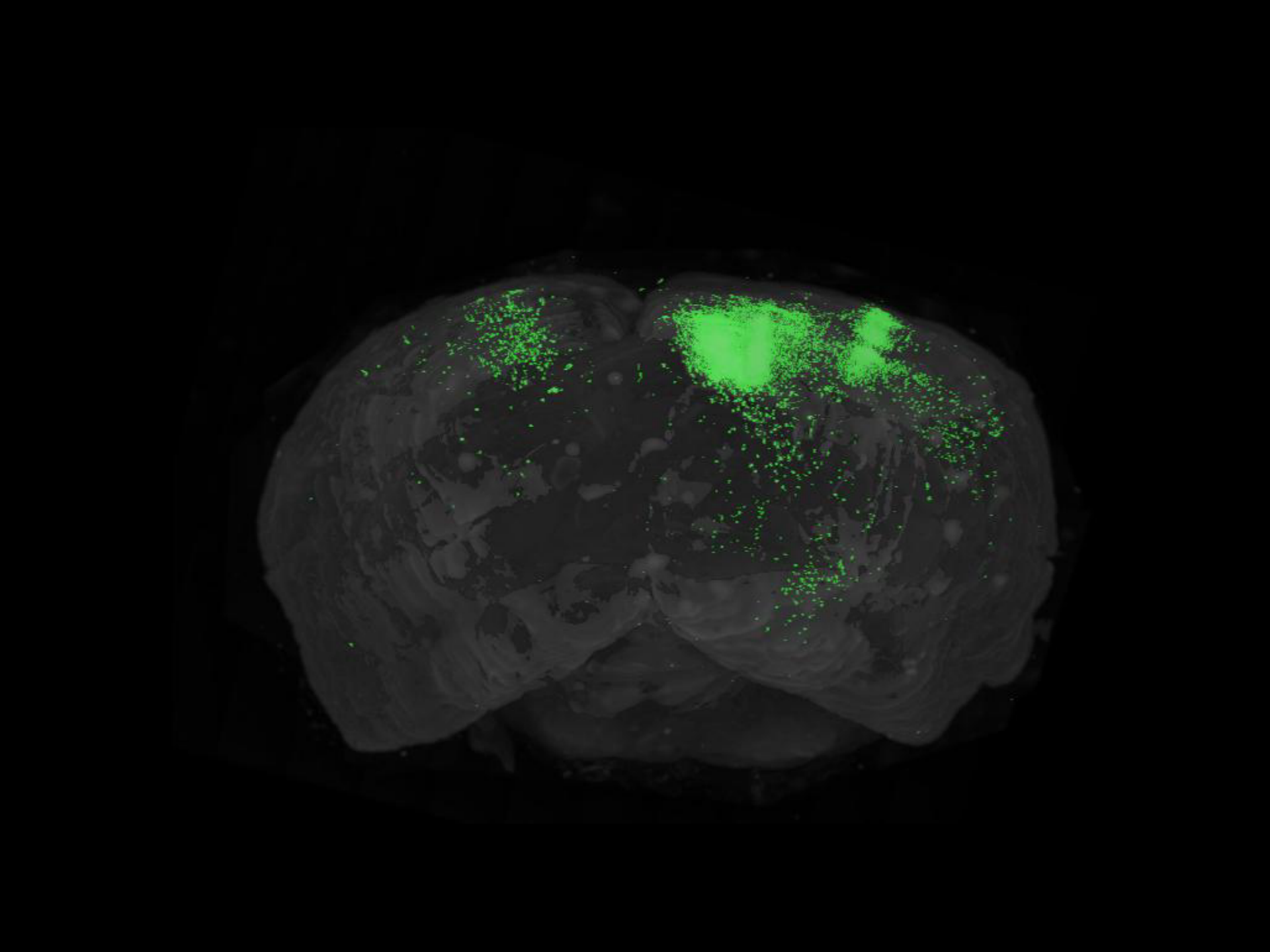

Grid-based ("Shotgun") approach to whole brain circuit mapping

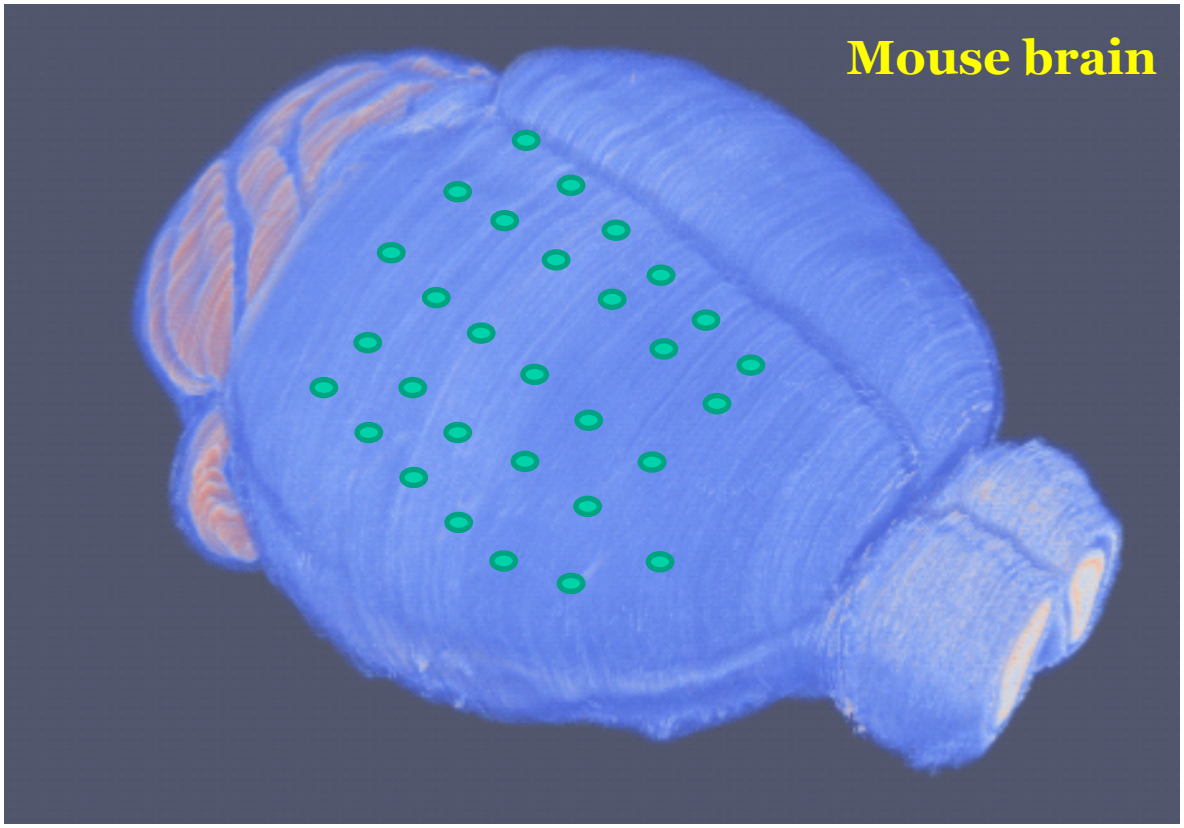

Grid ~1000 um

Total grid points
N = 380

Cortex (iso/paleo/archi)
N = 220

Other
N = 160

Algorithmic choice of coordinates for injections into the brain: encoding neuroanatomical atlas on a grid. (Grange *et al. 2011)*

MBA Pipeline

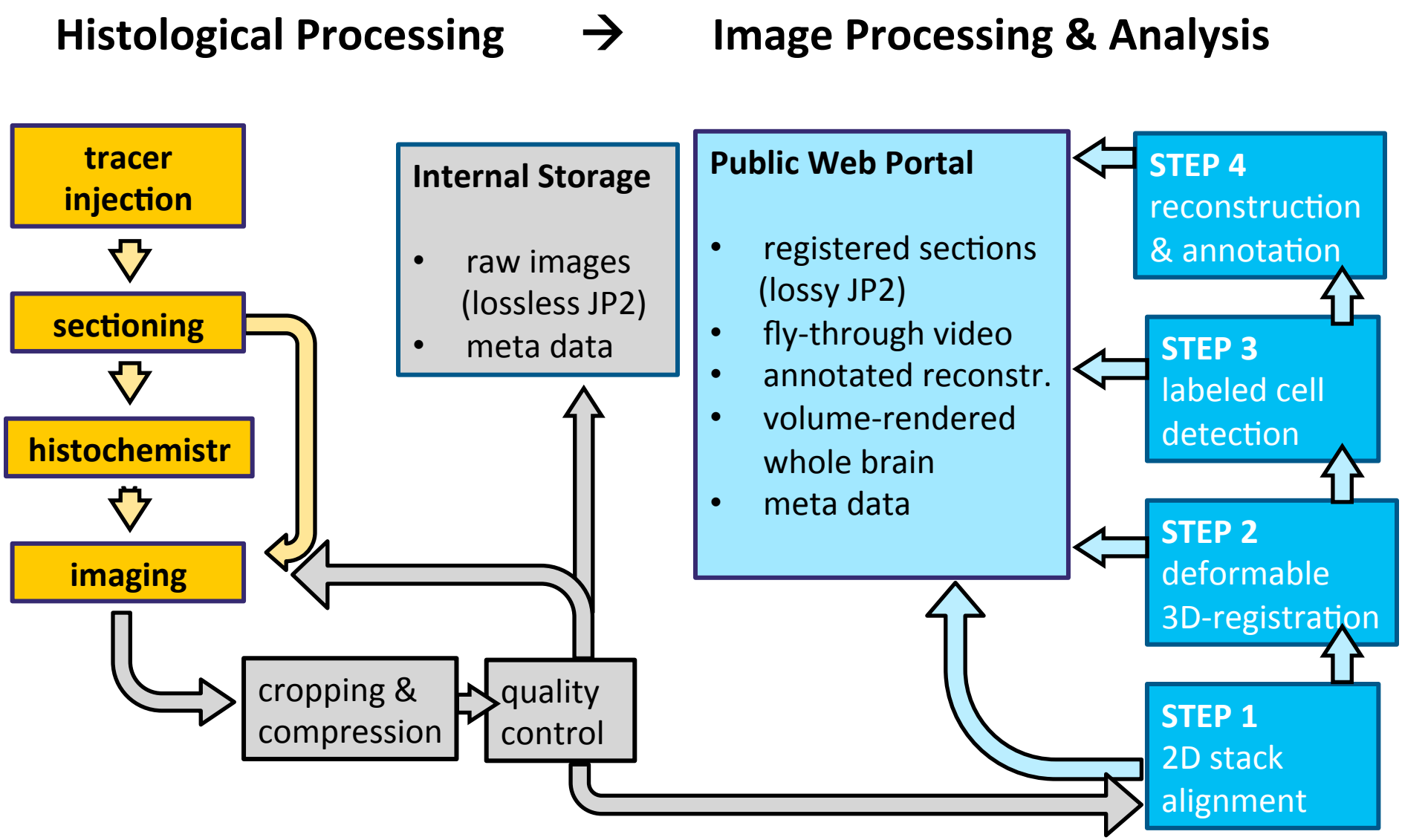

Key enabler: consumer electronics driven efficiency in the semiconductor industry, a.k.a. Moore's law (falling storage costs)

- 1 Mouse brain @1mu (LM) ~1TB
- 1000 Mouse brains @1mu ~1PB
- 1 Human brain @1mu ~1PB
- 1 Mouse brain @10nm (EM) ~ 1000PB

- 1TB in hard disk storage c. 1990 (inception of Decade of the Brain) 10M$
- Project data store currently 1PB (would have cost 10B$ in 1990).

a·nat·o·my

Origin

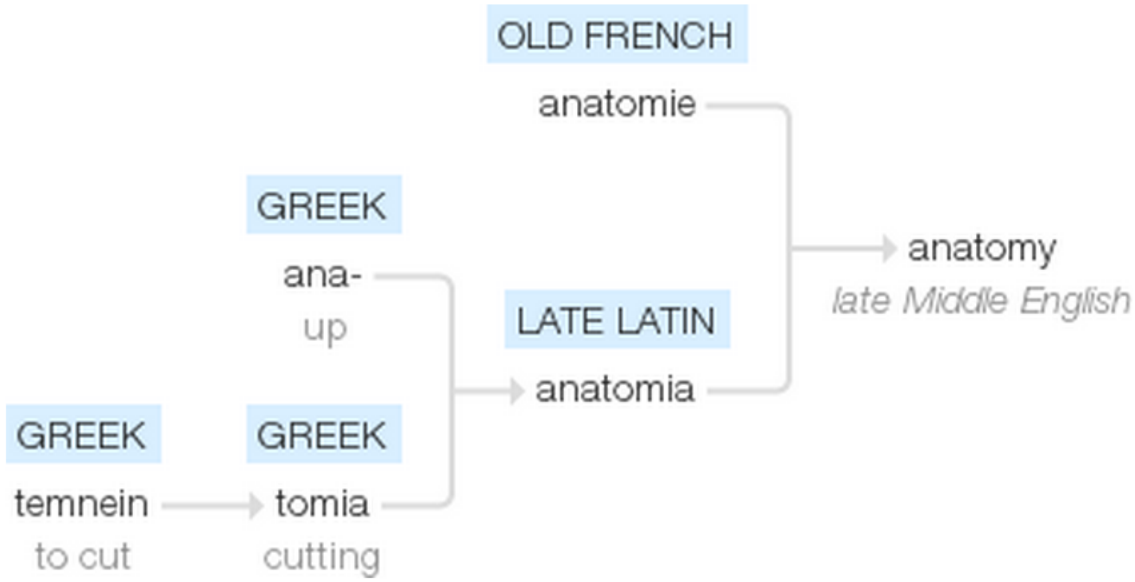

late Middle English: from Old French *anatomie* or late Latin *anatomia*, from Greek, from *ana-* ‘up’ + *tomia* ‘cutting’ (from *temnein* ‘to cut’).


Step 1


Step 2

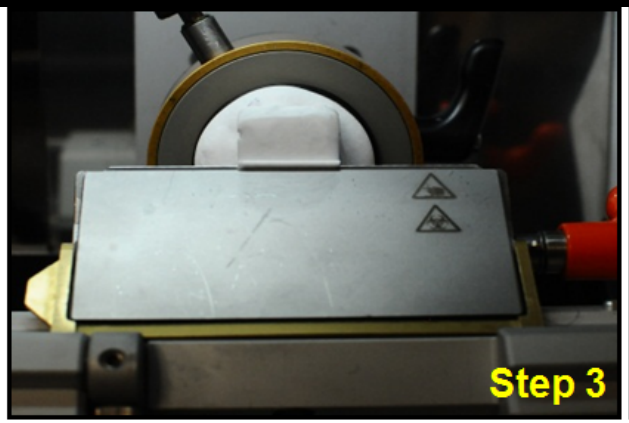
Step 3

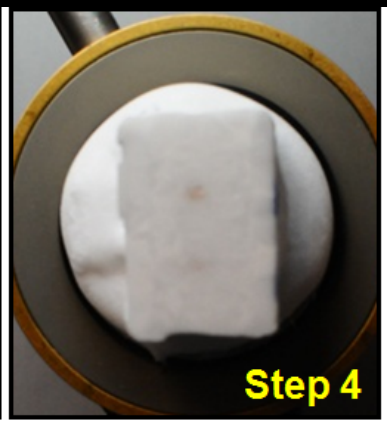
Step 4

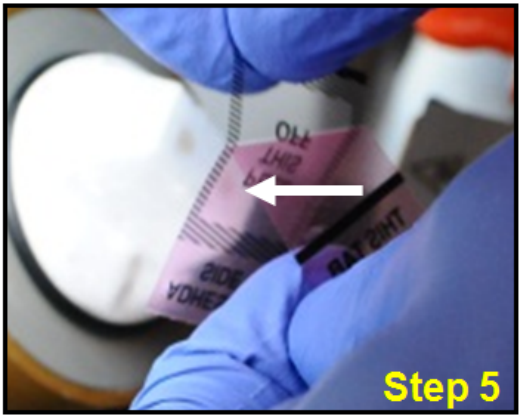
Step 5


Step 6


Step 7


Step 8

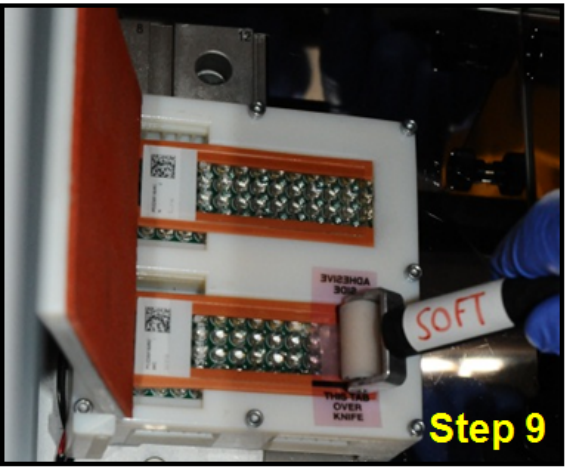
SOFT
Step 9


Step 10

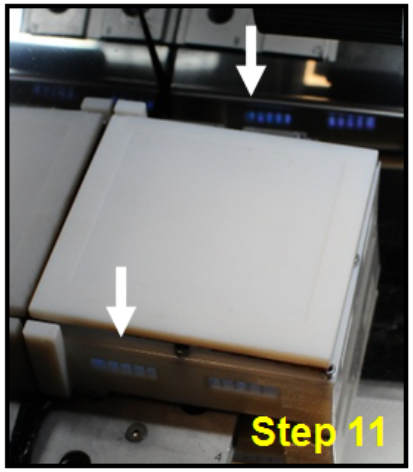
Step 11

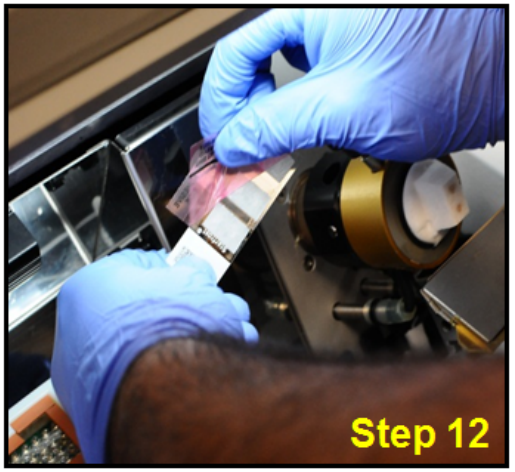
Step 12

MRI

Tape-transfer cut Coronal Nissls registered + virtually resectioned

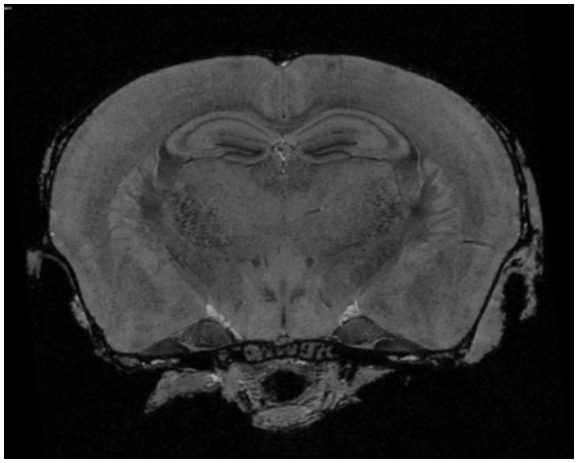

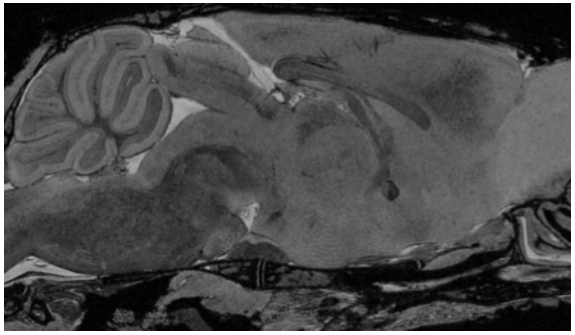

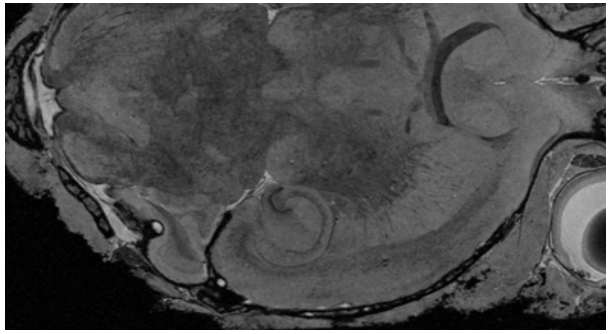

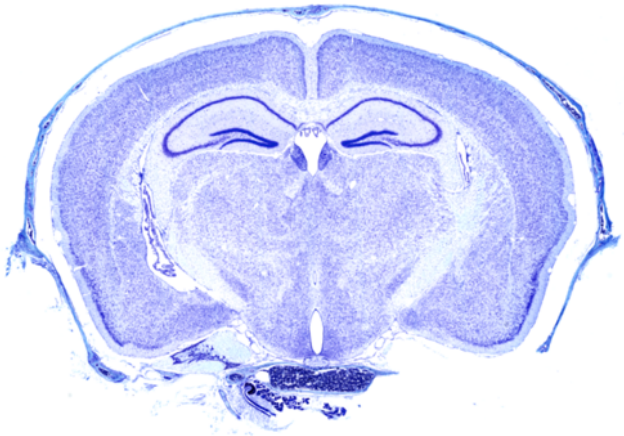

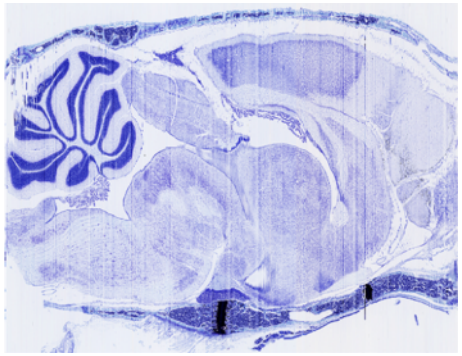

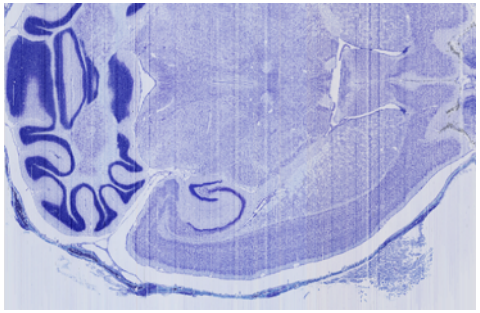

Registered Nissl Stack, 3D rendering showing surface vessels

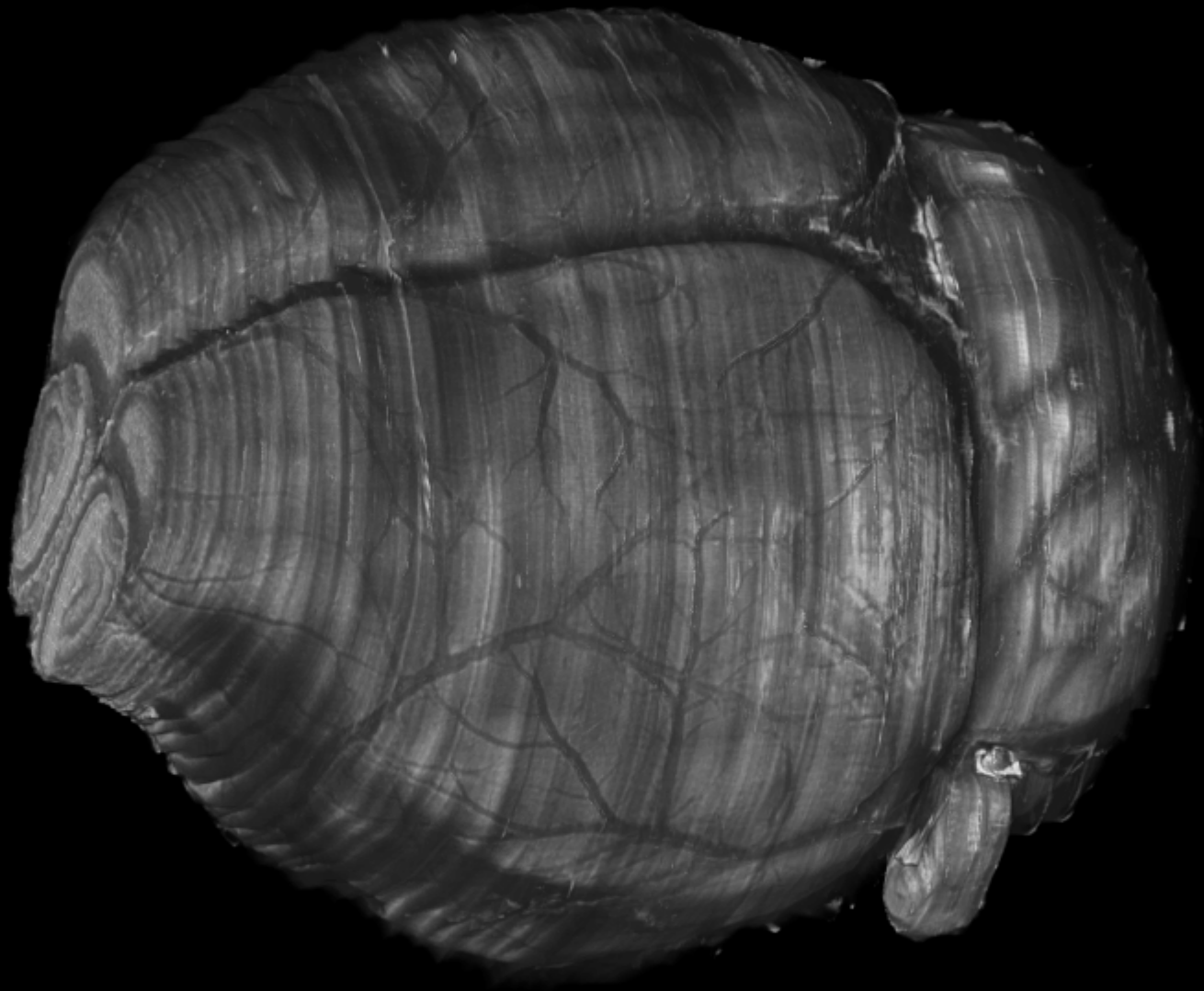

Image data

- Specimen size: ~1 centimeter
- Image resolution: 0.46 microns
- Section Spacing: 20 microns
- Ordering: Alternate Nissl
- Raw data: ~1TeraByte/brain
- # scanned: **~2000**
- Data size: Over 1PB.
- #sections: ~1 million (preserved on slide).

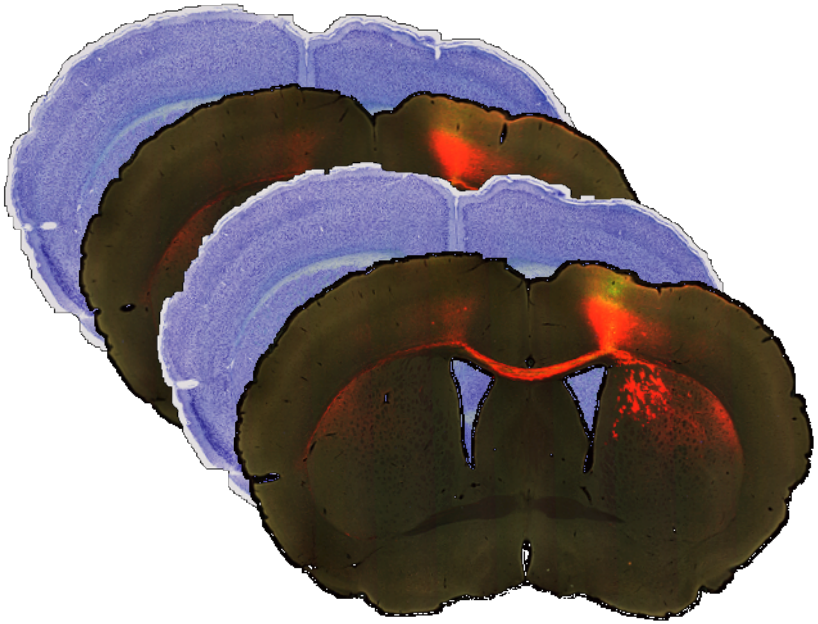

Fluorescent + Nissl series

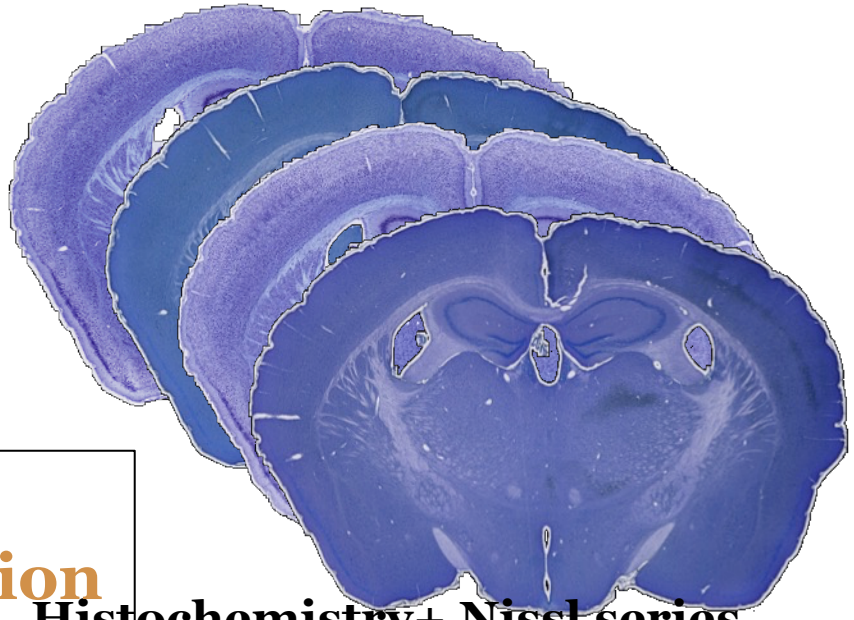

Histochemistry+ Nissl series

Alternate Cytoarchitecture And Connectivity information

Mouse Connectivity Mapping: Project Status Breakdown by tracer

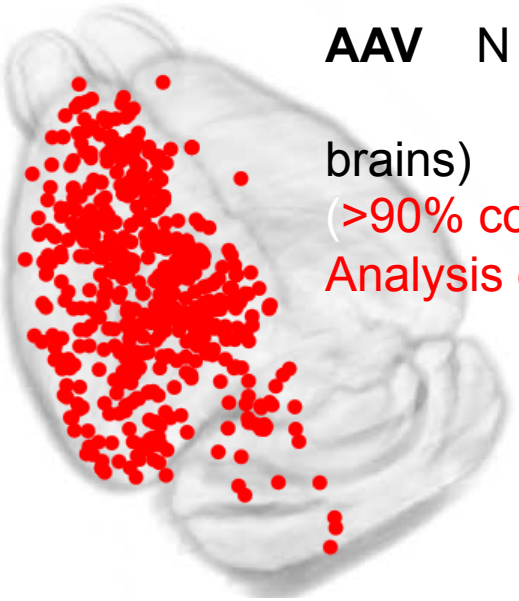

AAV N = 761 total (**527** brains)
(>90% complete; Analysis ongoing)

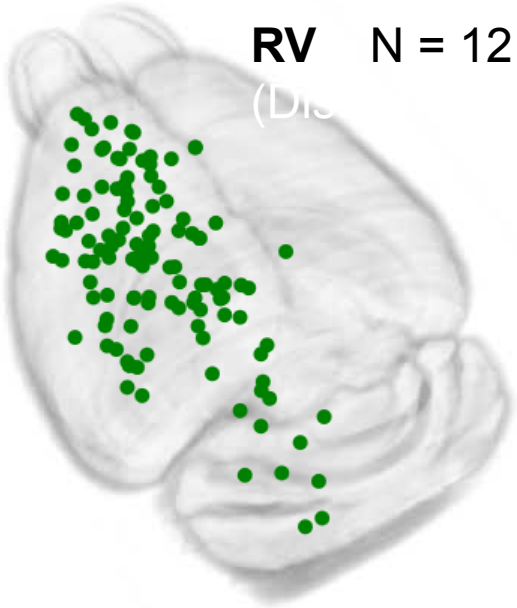

RV N = 121 total
(Di

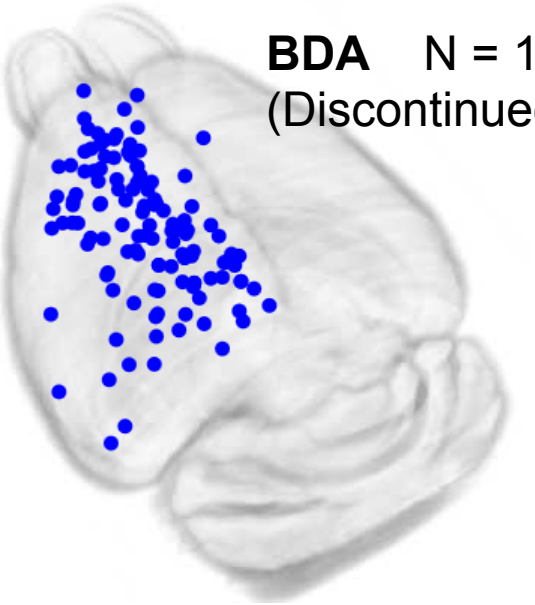

BDA N = 124 total
(Discontinued)

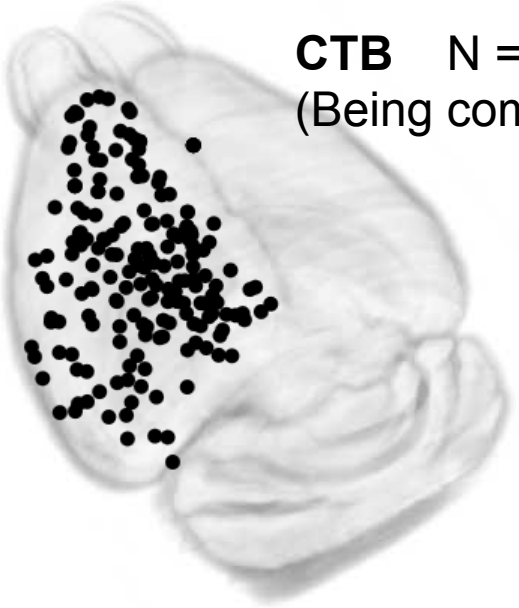

CTB N = 200 total
(Being completed)

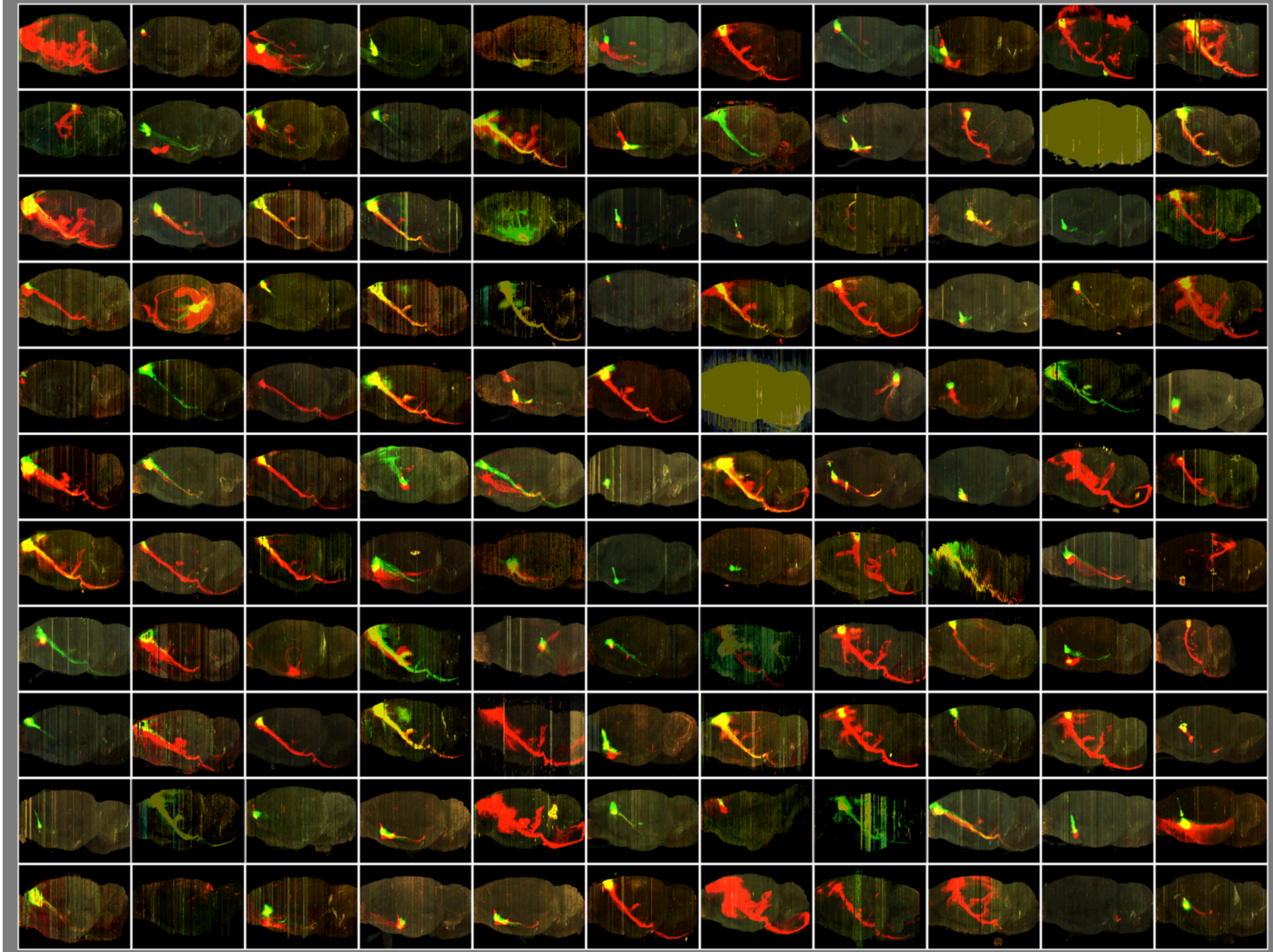

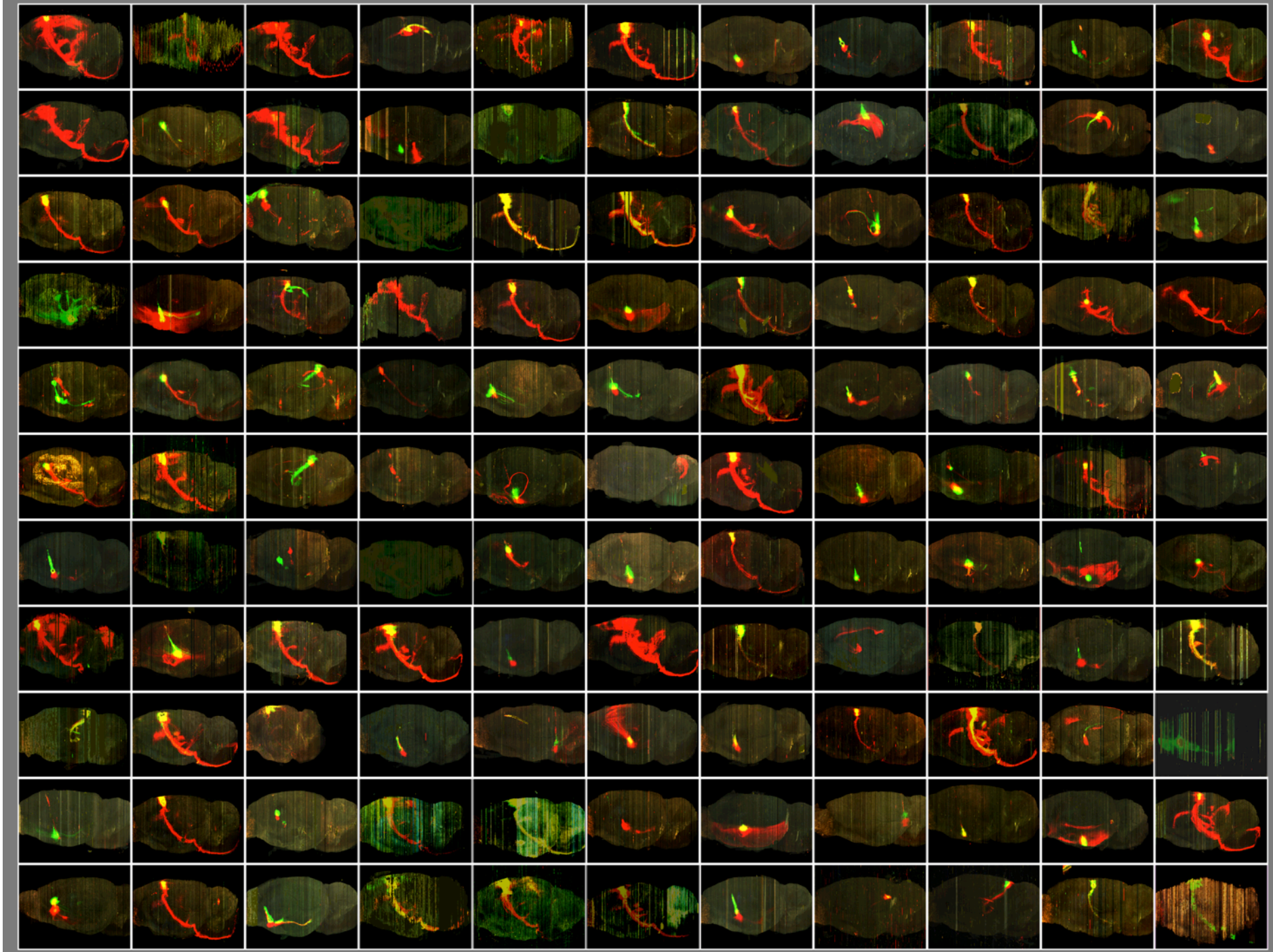

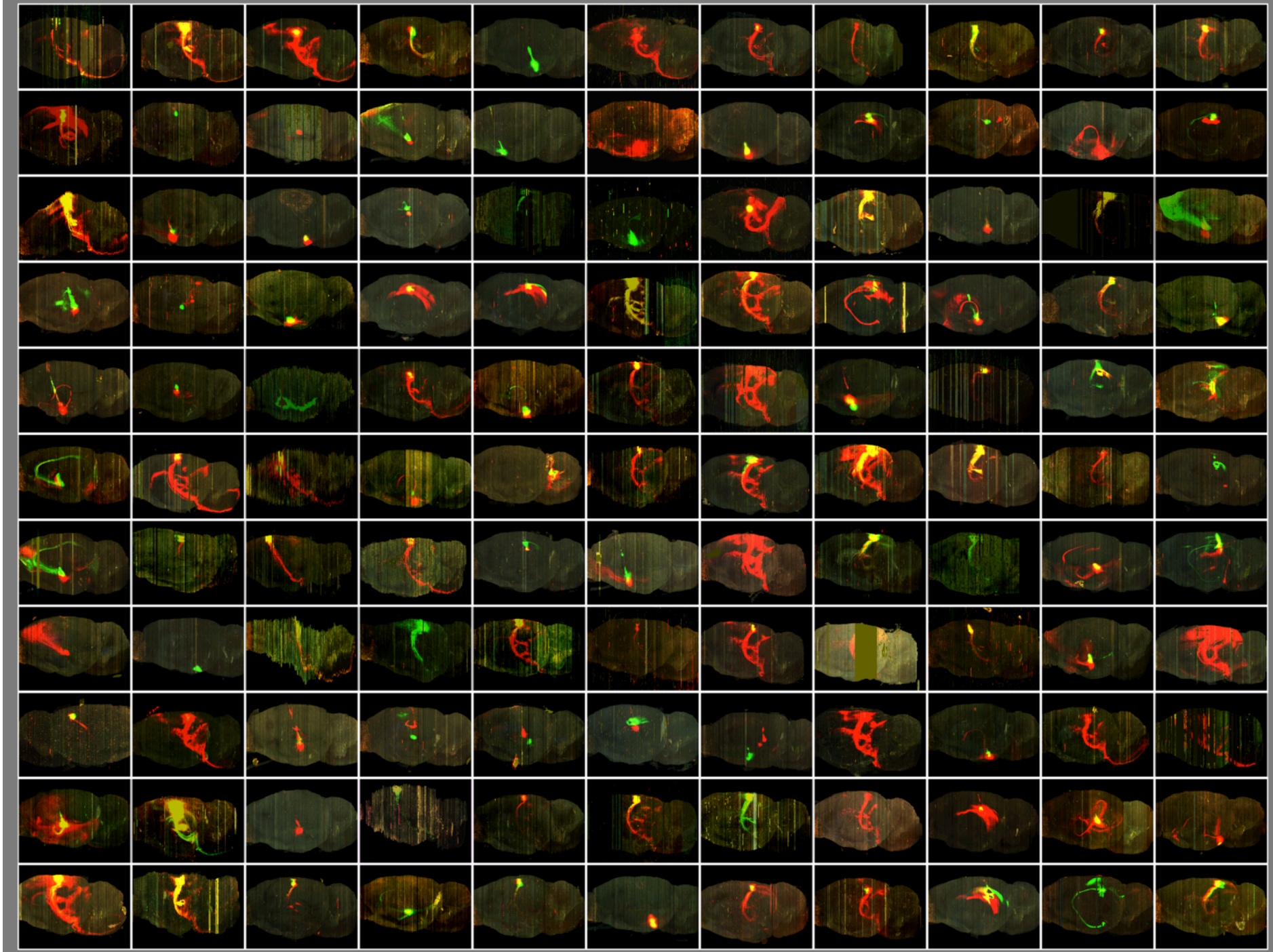

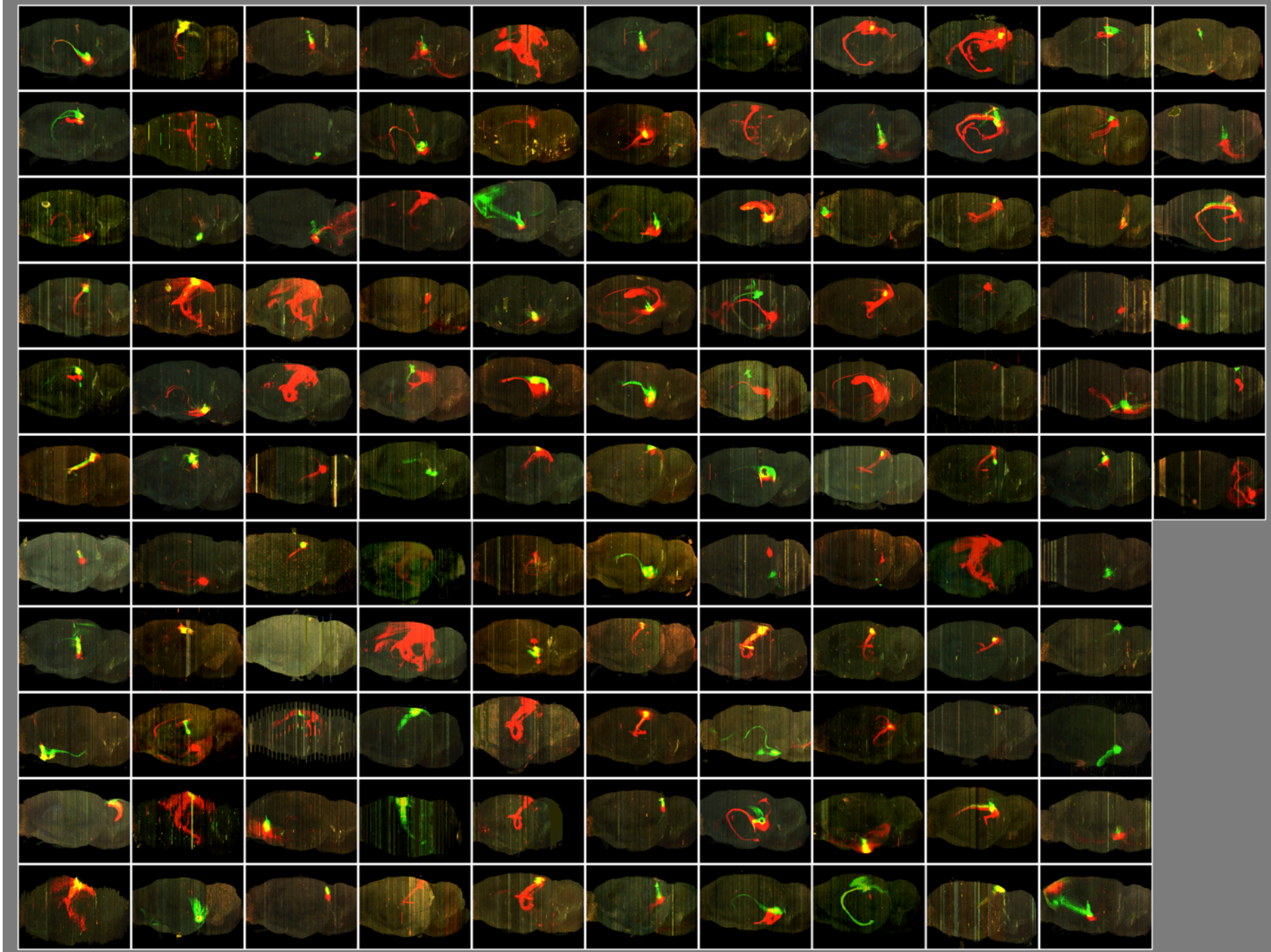

DATA PORTAL

HTTP://MOUSE.BRAINARCHITECTURE.ORG

MOUSE BRAIN ARCHITECTURE

MOUSE HOME | INJECTIONS: 3D VIEW | INJECTIONS: LIST VIEW | AUXILIARY DATASETS | DOCUMENTATION | EDUCATIONAL UNITS

3D Viewer

GET STARTED: Select your injection point below by clicking on the button to the right. Once an injection point is selected you will be brought back up to the 3D navigation. Click on the injection point to see a list of brains which will appear in the right hand column.

~850 tracer injected brains
~500 sections per brain
~ 0.5M high-resolution sections

CLEAR INJECTION POINTS

SELECT YOUR INJECTION POINTS

FILTER BY TRACER

FILTER BY REGION

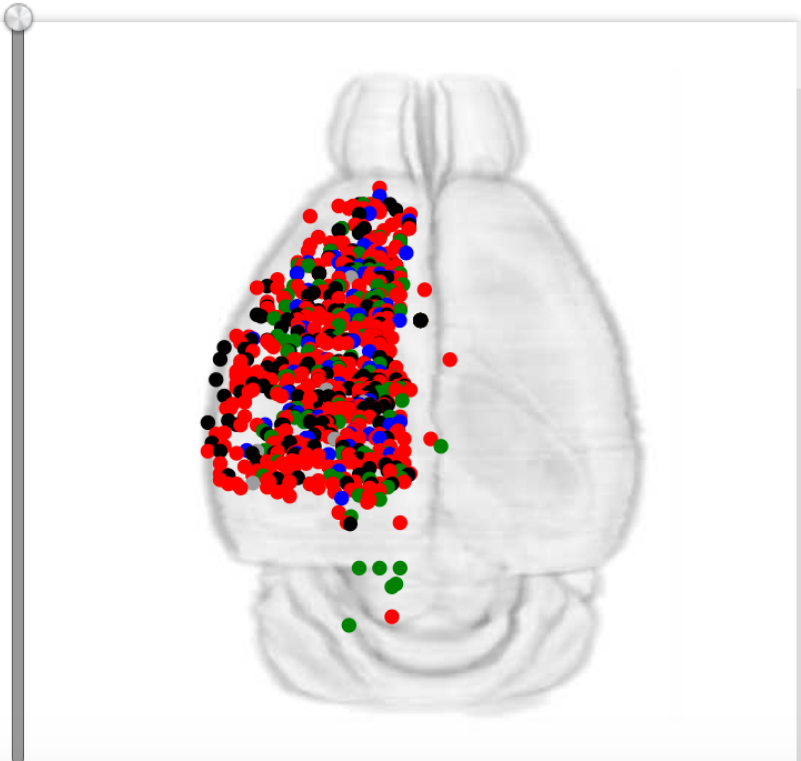

Brains Featured in this Area

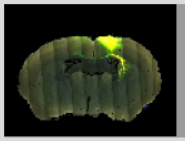

MouseBrain_1027 F
Inj Region : Primary motor area
Coordinates : (1.25 mm, -0.48 mm, 0.75 mm)
Tracer : AAV2/1 CAG

LEARN MORE | VIEW IMAGE | SECTION GALLERY | PLAY VIDEO

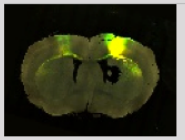

MouseBrain_0788 F
Inj Region : Primary motor area
Coordinates : (1.70 mm, 0.24 mm, 1.10 mm)
Tracer : AAV2/1 CAG

LEARN MORE | VIEW IMAGE | SECTION GALLERY | PLAY VIDEO

MouseBrain_0945 F
Inj Region : Primary motor area
Coordinates : (1.10 mm, -0.38 mm, 1.00 mm)
Tracer : AAV2/1 CAG

LEARN MORE | VIEW IMAGE | SECTION GALLERY | PLAY VIDEO

Data Analysis (Ongoing)

- Automatic detection of labelled cells and processes in the whole brain; Estimation of cell/process density
- Construction of a high-resolution Nissl-based reference atlas registered to postmortem (‘in vivo’-like) MR scans
- Comparison with literature
- Inference of collateral branching patterns

Labeled Cell detection:
graph based segmentation

Cells retrogradely labeled with CTB in nuclei of the dorsal thalamus. A) LD and (B) RE

These neurons project to the site of the injection in the association cortex (PTLp) ~ 1 mm caudal to this coronal section)

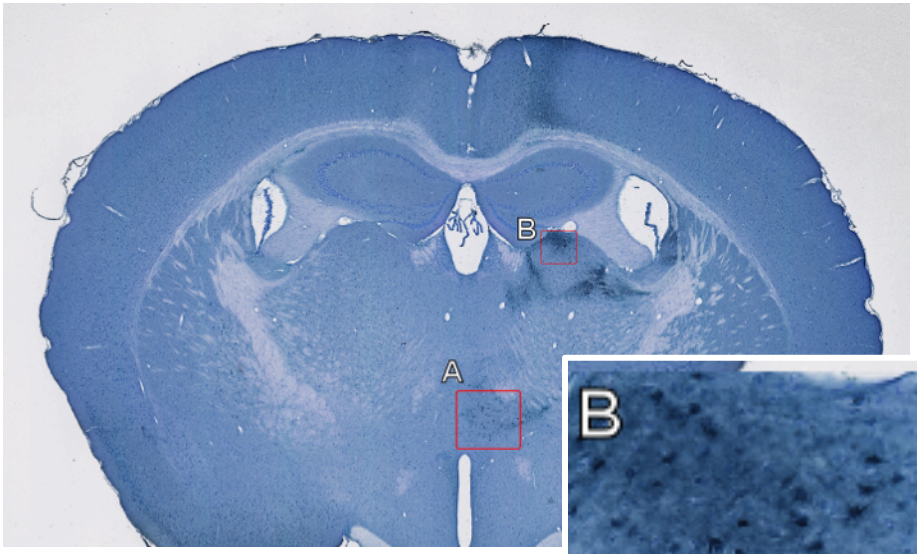

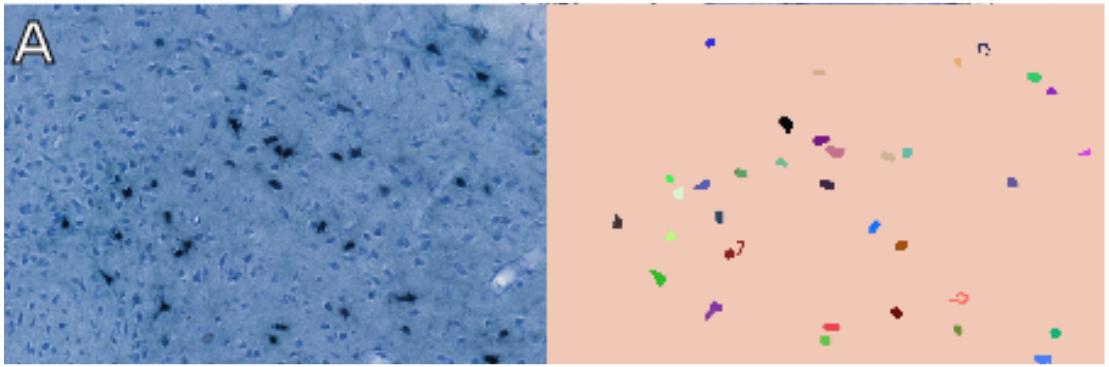

Labeled Process detection:
contrast enhancement for elongated structures, followed by gray-scale skeletonization

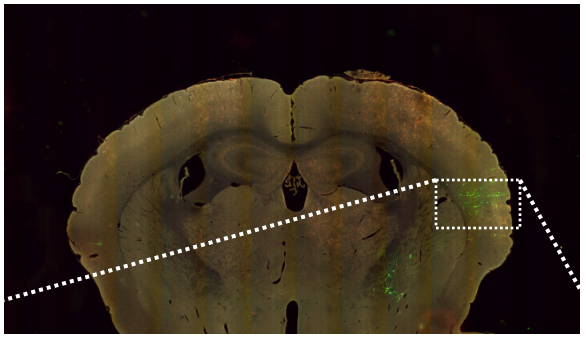

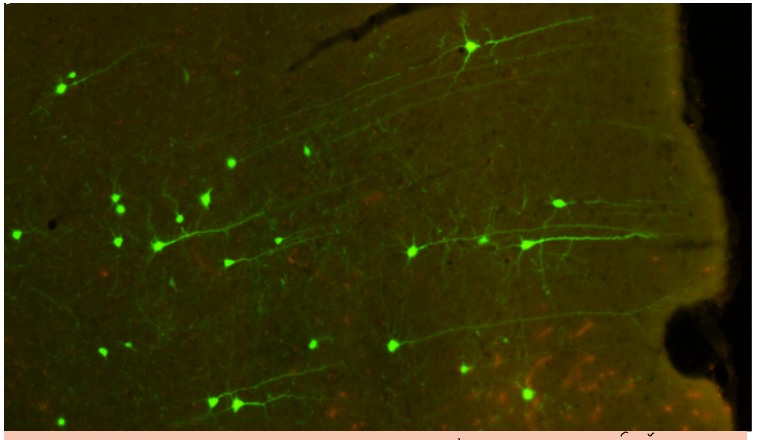

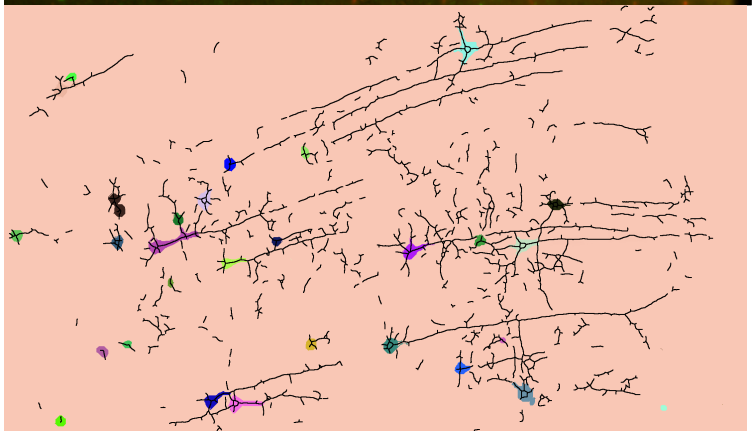

Cells in the secondary somatosensory cortex (SSs) expressing recombinant GFP in their dendrites & soma were infected with the retrograde virus tracer RV at their axon terminals that project to the primary somatosensory cortex (SSp; ~1.5 mm rostral to the coronal section shown), the site of the RV injection .

Counting Cells (Estimating Spatial Densities). Example: Counting GABAergic Cells

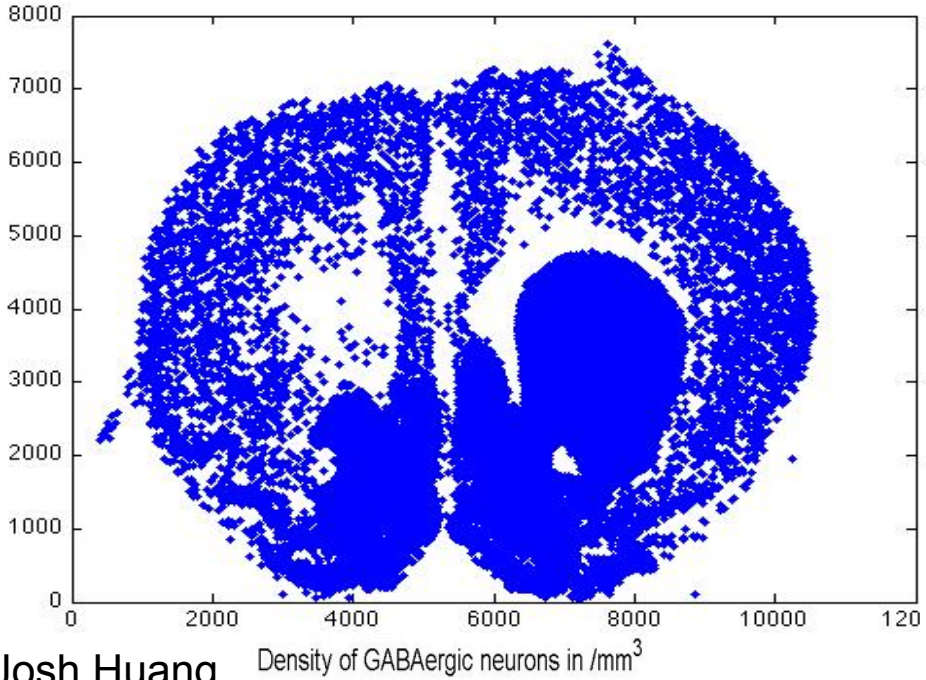

Josh Huang
Swagatam Mukhopadhyay
Zach Collins

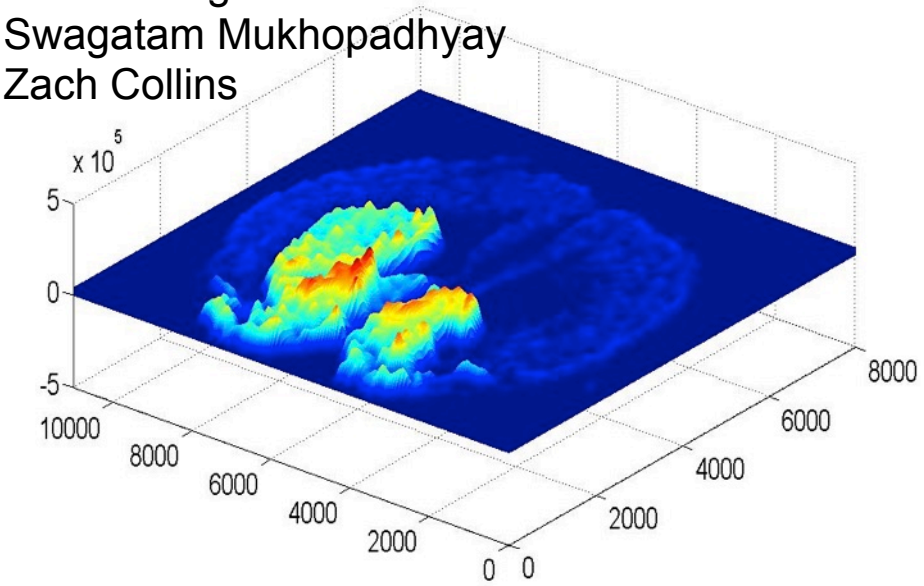

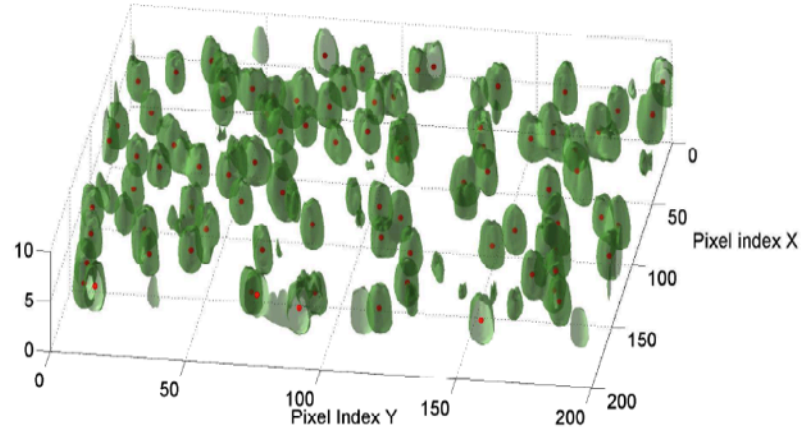

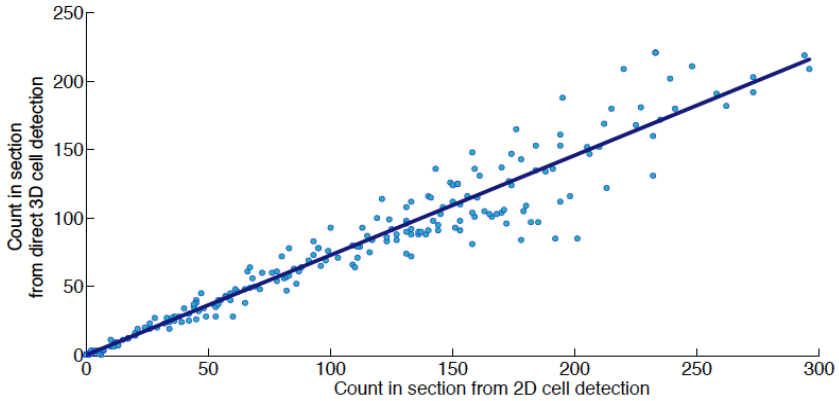

- We get 1-33 x10^3 /mm^3 in cortex (location dependent)
- Meyer et. al. [PNAS 108, 16807 (2011)] 3.5-14 x 10^3 /mm^3 in Ssp in Rat

Atlas “mapping”

The “**where problem**”.
Bringing the brain images to a **common reference**.

Addressed by taking structural
clues from the alternate Nissl series

Natural density clusters of cell-bodies

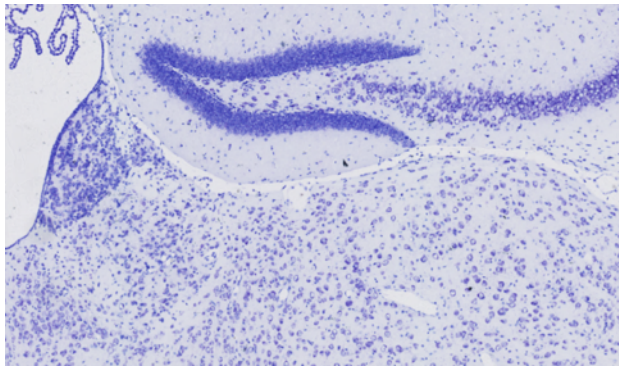

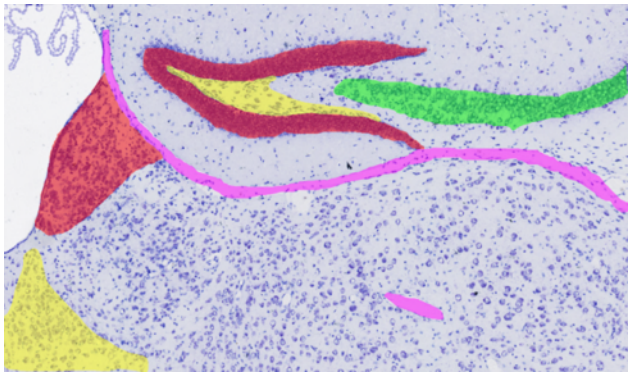

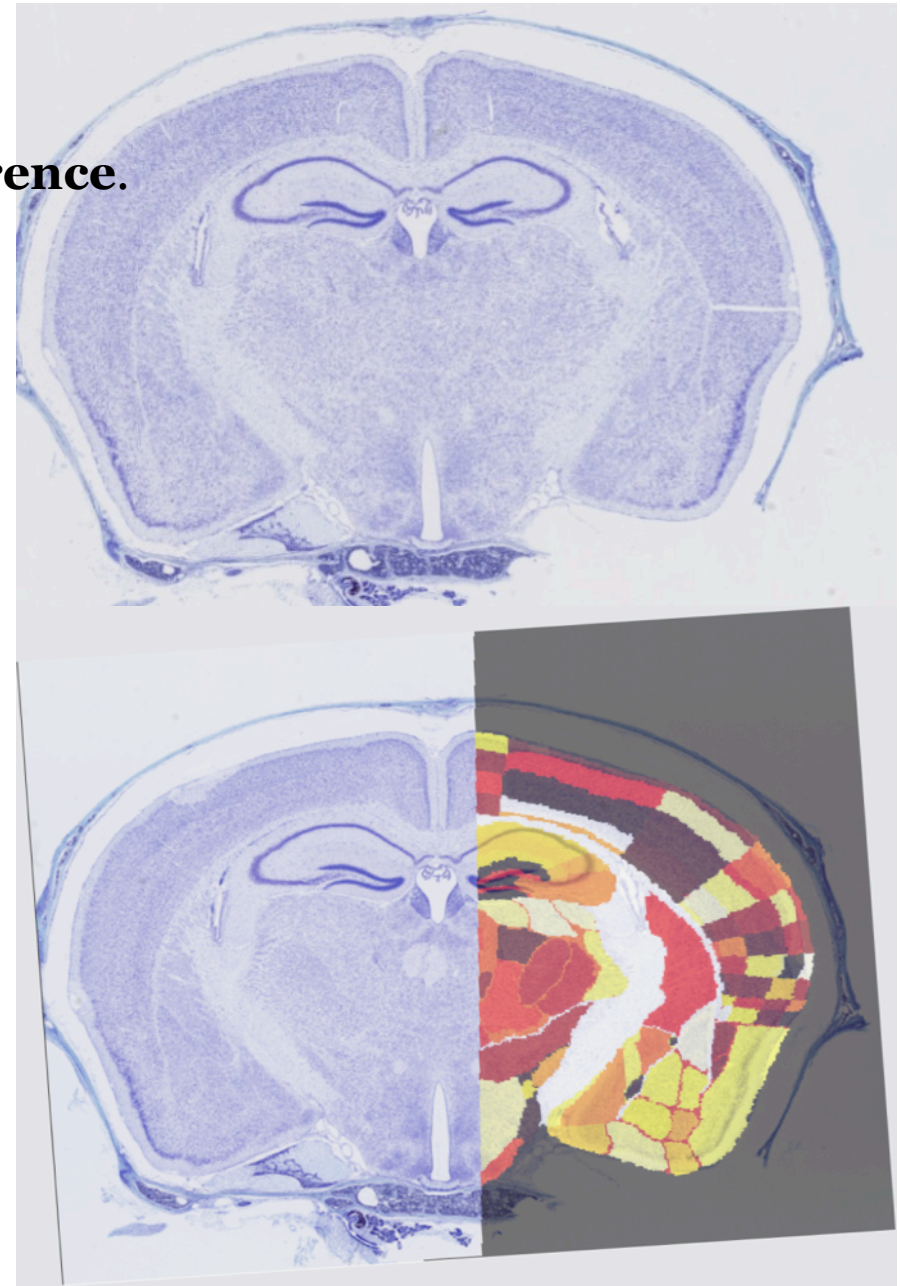

Ongoing analysis example: Skeletonization of projection data using Computational Topology

Collaboration with Yusu Wang, OSU

1-Stable manifold (collection of lines connecting maxima to saddles, ie mountain ridges separating neighboring valleys) Computed using the Discrete Morse Complex (combinatorial algorithm with ~linear time) + Persistence based simplification

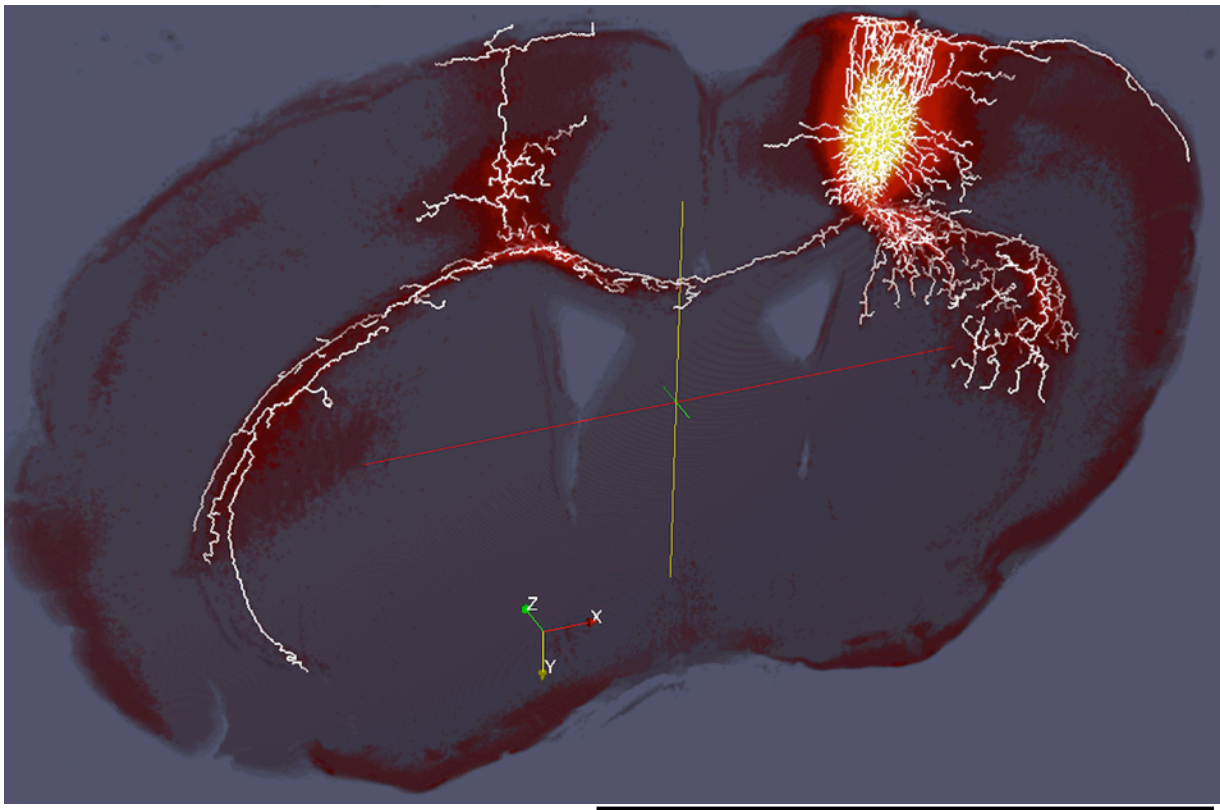

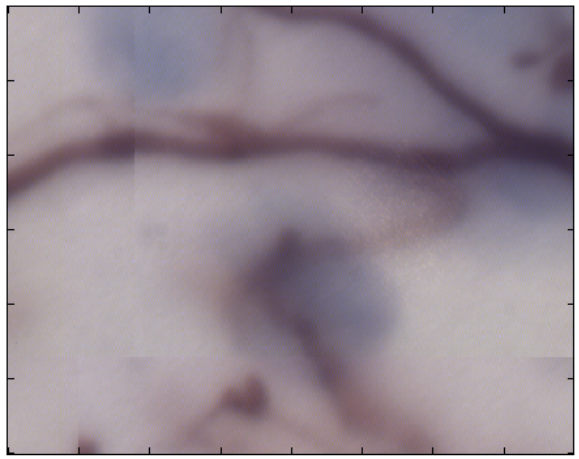

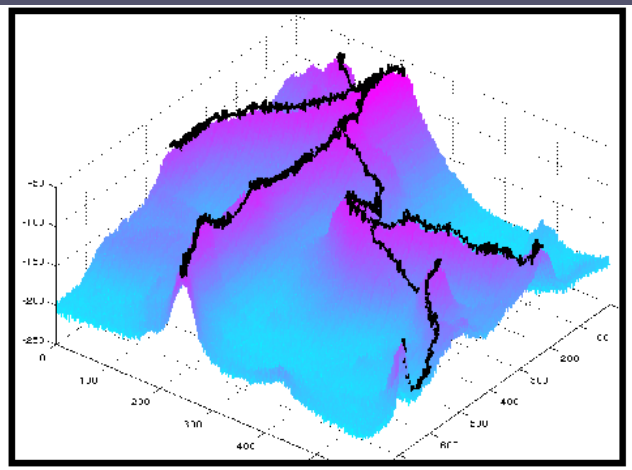

COMPARING WITH LITERATURE

Data Validation: Manual annotation (Courtesy Mihail Bota, USC)

MouseBrain_1035 HC	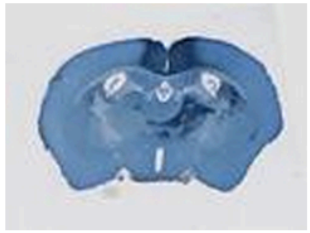	Primary motor area	x:0.83 y:-1.05 z:0.68	CTB
MouseBrain_1217 F	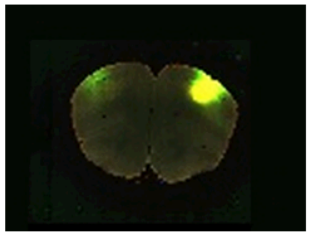	Primary motor area	x:2.20 y:1.70 z:1.75	AAV

78	RSPv	+++	++	Ipsi: a group of labeled neurons in the RSPv, close to the cing. Contra: same pattern, but weaker.
	RSPd	+++	++	Ipsi: strong labeling, especially towards the PTLp. Contra: moderate labeling, same pattern.
	PTLp	++		Ipsi: moderate/strong labeling. Contra: no discernible labeling.
	SSp	+++	+	Ipsi: strong labeling, in a general column-like pattern. Contra: a similar columnar pattern, but much weaker.
	AUDd	++		Ipsi: labeling of the entire cortex from the AUDd to TEa. The labeled neurons are in the deep layers. Contra: no labeling,
	AUDv	++		Ipsi: labeling of the entire cortex from the AUDd to TEa. The labeled neurons are in the deep layers. Contra: no labeling,
	AUDp	++		Ipsi: labeling of the entire cortex from the AUDd to TEa. The labeled neurons are in the deep layers. Contra: no labeling,
	TEa	++	+	Ipsi: labeling of the entire cortex from the AUDd to TEa. The labeled neurons are in the deep layers. Contra: no labeling,
	ECT	+	+	Ipsi: labeling of the entire cortex from the AUDd to TEa. The labeled neurons are in the deep layers. Contra: no labeling,
83	RSPv	++	+	Ipsi: weak/moderate labeling, stopping exactly where the SUBd starts. Contra: very weak labeling, 2-3 labeled neurons.
	RSPd	+++	++	Ipsi: clear band of labeled neurons in layer III. Also in the deeper layers. Moderate/strong labeling. Contra: same labeling
	RSPagl	++		Ipsi: weak-moderate labeling at best. Contra: no label.
	VISam	+		Ipsi: weak-moderate labeling at best. The neurons tend to be in layer V. Contra: no label.
	VISal	+		Ipsi: weak-moderate labeling at best. The neurons tend to be in layer V. Contra: no label.
	PTLp	+		Ipsi: weak-moderate labeling at best. The neurons tend to be in layer V. Contra: no label.
	AUDv	+		Ipsi: weak-moderate labeling at best. The neurons tend to be in layer V. Contra: no label.
	TEa	+	+	Ipsi: weak labeling. Contra: maybe some weakly labeled neurons

Manual annotation of 2 injections (Mihail Bota, USC)

Only “sensory-motor' cortical regions shown, superposed on a network in Rat (BAMS data, grey)

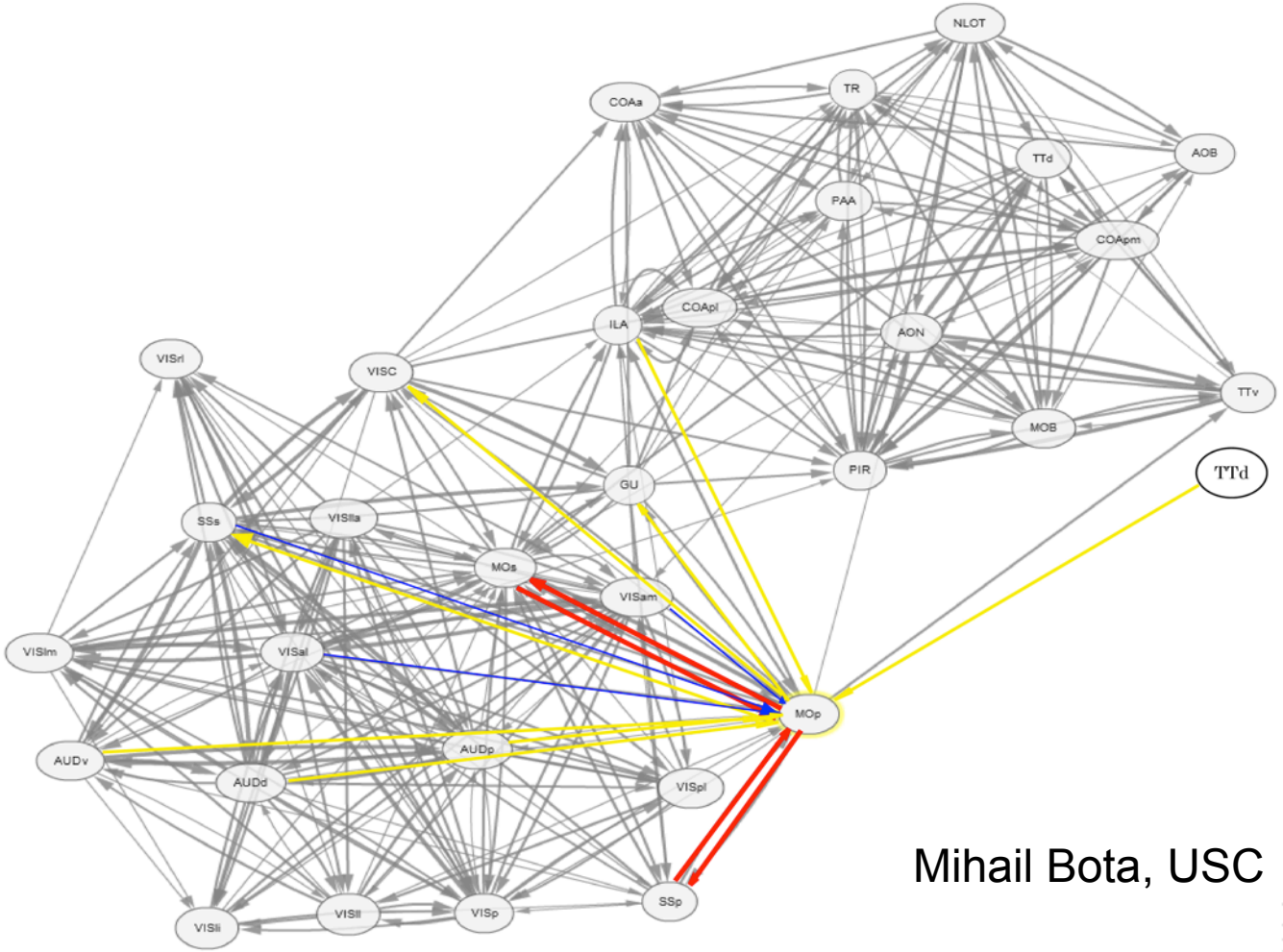

(1) CTB (retrograde) in primary motor cortex (Mop) – shown by incoming arrows.
(2) AAV (anterograde) in in primary motor cortex (Mop) – shown by outgoing arrows.

AIBS Cortex Connectivity Matrix

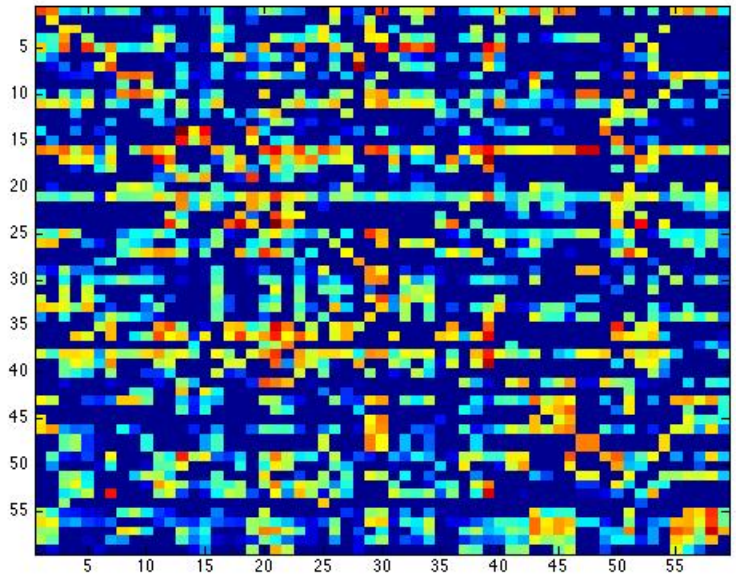

BAMS Cortex Connectivity Matrix

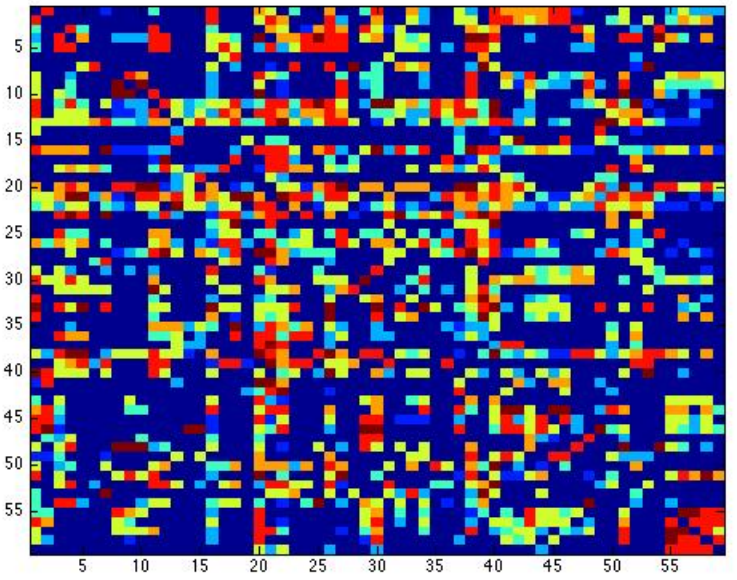

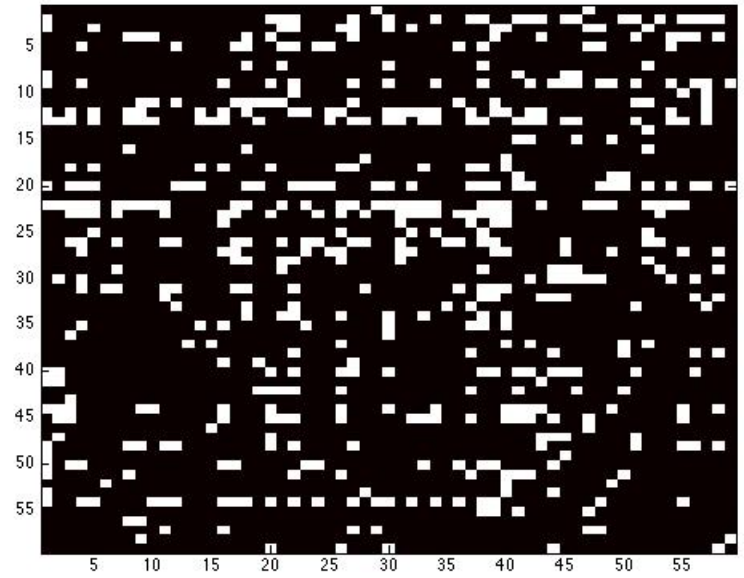

“False Negatives” (16%)

“False Positives” (14%)

Comparing regional output and input patterns of AIBS, BAMS matrices.

Null hypothesis – projections randomly chosen (preserving the distribution of weights)

- For outgoing projections: Null hypothesis of randomly chosen projections cannot be rejected for:
  - 95% level: 6/59 regions (10%)
    - 'AIv' 'ENTm' 'GU' 'ILA' 'ORBvl' 'PRE'
  - 99% level: 11/59 regions (19%)
    - 'ACAv' 'AIv' 'ENTm' 'EPd' 'GU' 'ILA' 'NLOT' 'ORBl' 'ORBvl' 'PRE' 'VISpl'
- For incoming projections:
  - 95% level: 2/59 regions (3%)
    - 'COAa' 'PRE'
  - 99% level: 14/59 regions (24%)
    - 'ACAv' 'AIp' 'CA2' 'COAa' 'DG' 'ILA' 'NLOT' 'ORBl' 'PAR' 'PERI' 'POST' 'PRE' 'SSp' 'TEa'

WHOLE BRAIN CIRCUIT MAPPING IN OTHER SPECIES:

MARMOSET (RIKEN, JAPAN)

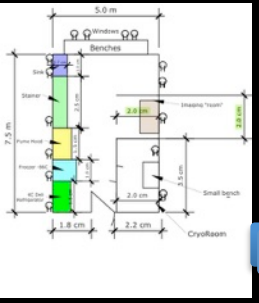

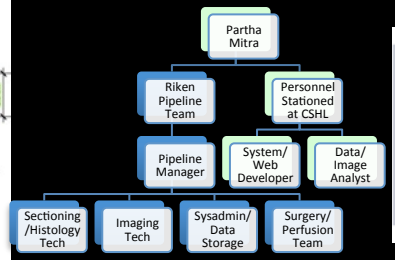

Lab/pipeline setup complete; Personnel hired; 7 Marmosets processed so far; on track to process 25 by March 2016

RIKEN Marmoset Brain Architecture
Lab: Copy of CSHL MBA lab (part of Japan Brain Science Initiative)
Collaboration with Hideyuki Okano, Atsushi Iriki, Erica Sasaki

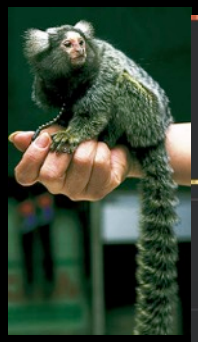

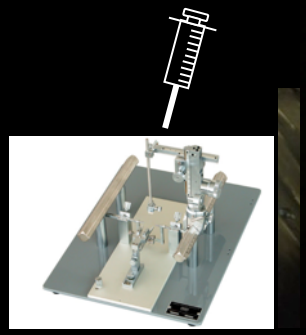

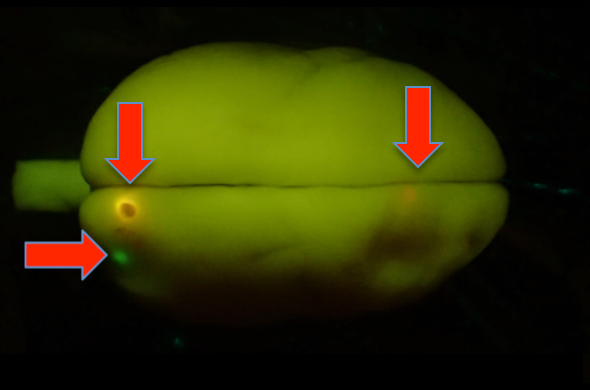

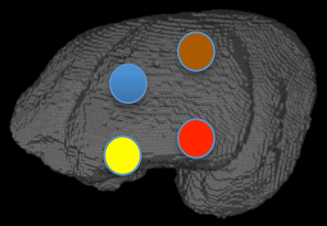

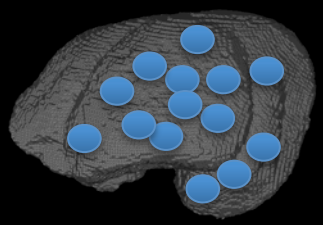

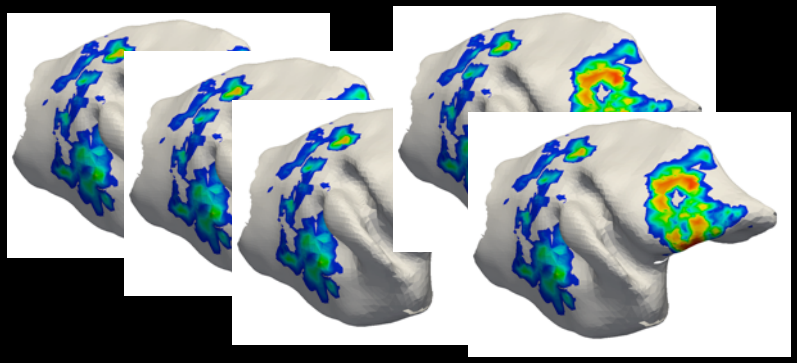

4-5 injections/brain
(2 color AAV/Anterograde)
(2 color retrograde fluorescent
+ 1 DAB/Brightfield CTB)

Brainwide Injection grid

In 2015 project year plan to inject 25 Marmosets x 4-5 injections each = 100-125 injections

II.

"Thermodynamics of Big Data"

Analysis of Algorithmic Phase Transitions in Compressed Sensing/Sparse Regression

NSF INSPIRE: Zero-One Laws at the Interface Between Physics, Engineering and Biology

Partha Mitra
Bassam Bamieh (UCSB)
Anirvan Sengupta (Rutgers)

Phase transitions
in statistical physics ..

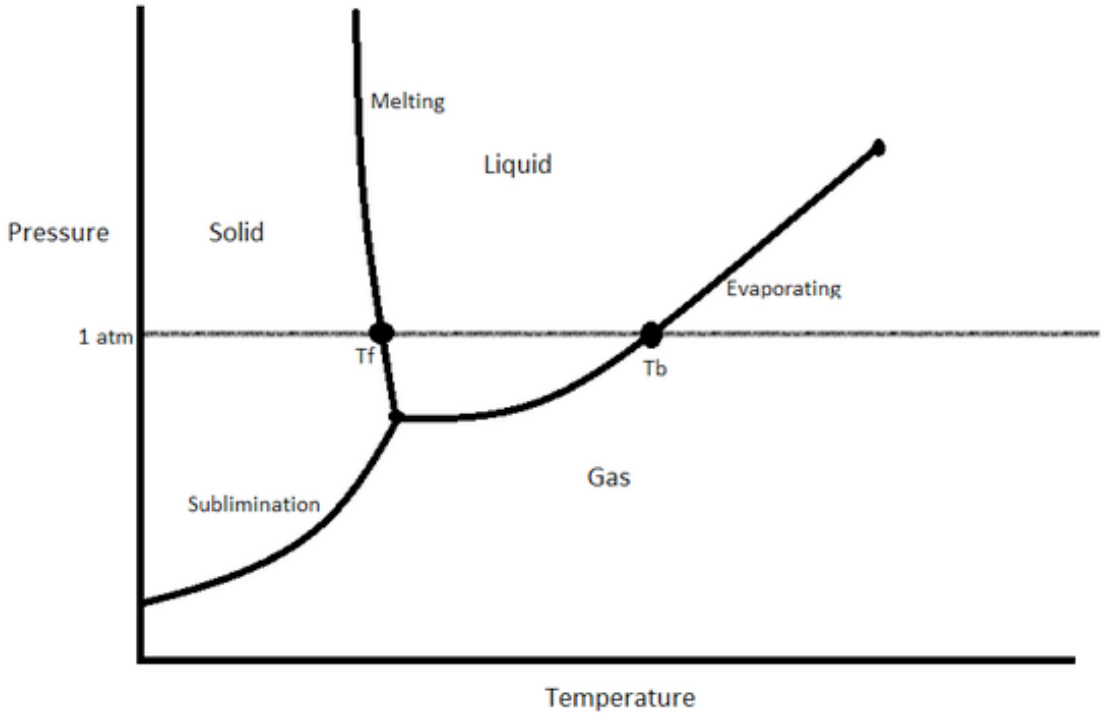

Typical solid-liquid-gas phase diagram showing sharp boundaries

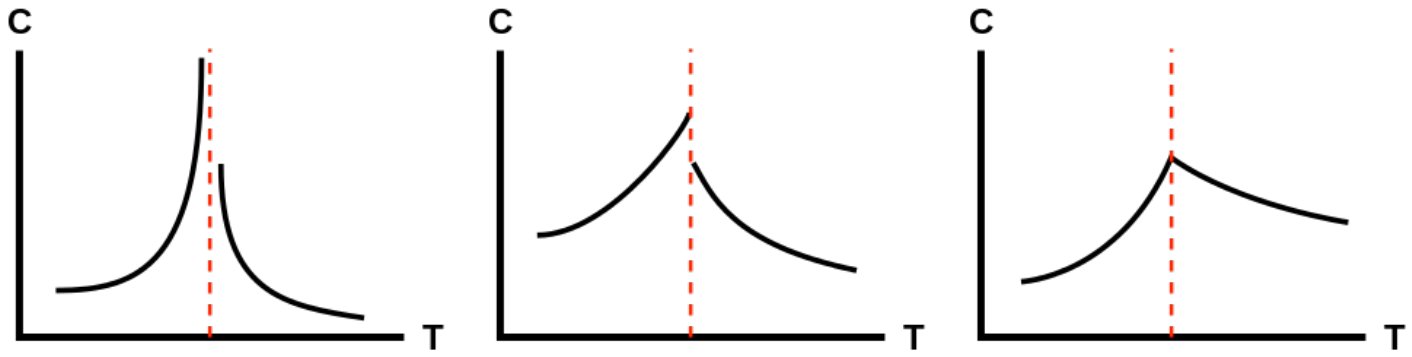

Jumps/divergences in thermodynamic quantities at transition points

Phase transitions in Statistical Physics

- Non-analytic behavior of the Free Energy in the large-N limit
- Ising model 1924
- Landau (Mean Field) theory 1937
- Onsager solution (2D Ising model) 1944
- Renormalization group theory: Kadanoff (1966); Wilson (1971); Fisher (1972)
- Spin glasses; Replicas; Edwards, Anderson (1975)

Phase transitions in Theoretical Engineering (Communications, Computation, Controls, Machine Learning)

- Consequence of large numbers of variables
- Shannon (sharp threshold for error correcting codes at rate = channel capacity) 1948
- Computation: k-SAT (satisfiability problems) "easy-hard-easy" phase transitions for the average case ~1990s [relevant for P vs NP]
- Machine learning examples ~1990s
- Communication networks ~1990s
- Distributed control theory ~ more recent

Communication Networks

Adv. Appl. Prob. **34,** 58–84 (2002)
Printed in Northern Ireland

MARKOV RANDOM FIELD MODELS OF MULTICASTING IN TREE NETWORKS

KAVITA RAMANAN * ** AND
ANIRVAN SENGUPTA,* *Bell Laboratories, Lucent Technologies*
ILZE ZIEDINS,*** *University of Auckland*
PARTHA MITRA,* *Bell Laboratories, Lucent Technologies*

Abstract

In this paper, we analyse a model of a regular tree loss network that supports two types of calls: unicast calls that require unit capacity on a single link, and multicast calls that require unit capacity on every link emanating from a node. We study the behaviour of the distribution of calls in the core of a large network that has uniform unicast and multicast arrival rates. At sufficiently high multicast call arrival rates the network exhibits a 'phase transition', leading to unfairness due to spatial variation in the multicast blocking probabilities. We study the dependence of the phase transition on unicast arrival rates,

Distributed Controls

Bamieh, Bassam, Mihailo R. Jovanovic, Partha Mitra, and Stacy Patterson.
"**Coherence in large-scale networks: Dimension-dependent limitations of local feedback**."
Automatic Control, IEEE Transactions on 57, no. 9 (**2012**): 2235-2249.

Vehicular Platoons

Automated control of each vehicle, tight spacing at highway speeds

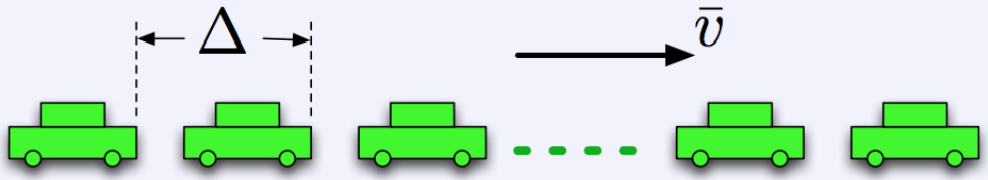

- Is it enough to look at neighbors? What to broadcast to all?
- What happens in the presence of disturbances?
- How does performance scale with size?
- Are there any fundamental limitations?

Machine Learning

Ramezanali, Mohammad, Partha P. Mitra, and Anirvan M. Sengupta.

"**The cavity method for phase transitions in sparse reconstruction algorithms**." arXiv preprint arXiv:1501.03194 (2015).

"**Critical behavior and universality classes for an algorithmic phase transition in sparse reconstruction**." *arXiv preprint arXiv:1509.08995* (2015).

Erlich, Yaniv, Assaf Gordon, Michael Brand, Gregory J. Hannon, and Partha P. Mitra. "**Compressed genotyping**." *Information Theory, IEEE Transactions on* 56, no. 2 (2010): 706-723.

Motivation/Relevance to brains

- Big data sets (eg large neuroanatomical data cubes) -> to understand the data analysis methods.
- "Deep networks" etc: theoretically poorly understood, need analytical tools.
- Why does the brain have so many neurons?
  - Is the brain solving "big data" problems?
  - Does the micro-network architecture involve phase transition phenomena in interesting ways?

Case Study:
Thresholding parameters in Multivariate Regression
(especially when # parameters > # samples)

- $Y = H x + n$
- Classical method:
  - Minimize MSE: $X = \text{argmin}_x |Y-Hx|^2 = H^* Y$, where H^* is the pseudoinverse of H
  - Keep only the largest, statistically significant regressors: a hard threshold: $X = Th(H^* Y)$
  - Threshold determined e.g. by computing F-ratio test for residuals (variety of procedures available).

A popular current approach: Regression with sparsity inducing penalties

- Basis Pursuit (Chen, Donoho, Saunders 1999; Tibshirani 1996)
  - $X=\text{argmin}_x |Y-Hx|^2+\lambda|x|$

- Can be regarded as convex relaxation of non-convex, NP hard problem with penalty = number of non-zero components.
- Guarantees recovery of correct solution for zero noise, for sufficiently sparse vectors, in the limit $\lambda->0$.
- Solved efficiently using linear programming.
- "Good" and "Bad" phases (recovery possible/not possible) separated by phase transition boundary with analytically known form (Donoho 2006)

- History: Prony's method for recovering multiple sinusoids (1795). L1 minimization for sparse frequency estimation (Logan, 1965)

$$Y = H X$$

Y : m-dimensional measurement vector
H : m x N dimensional (known) design matrix
X : N-dimensional sparse parameter vector,
with only s non-zero entries

Sparsity parameter $\rho = s/N$
Undersampling parameter $\alpha = m/N$

Combinatorial algorithm recovers if $s<m$ ($\rho < \alpha$)
Transition line for the combinatorial (exponentially costly) algorithm is the diagonal line $\rho = \alpha$

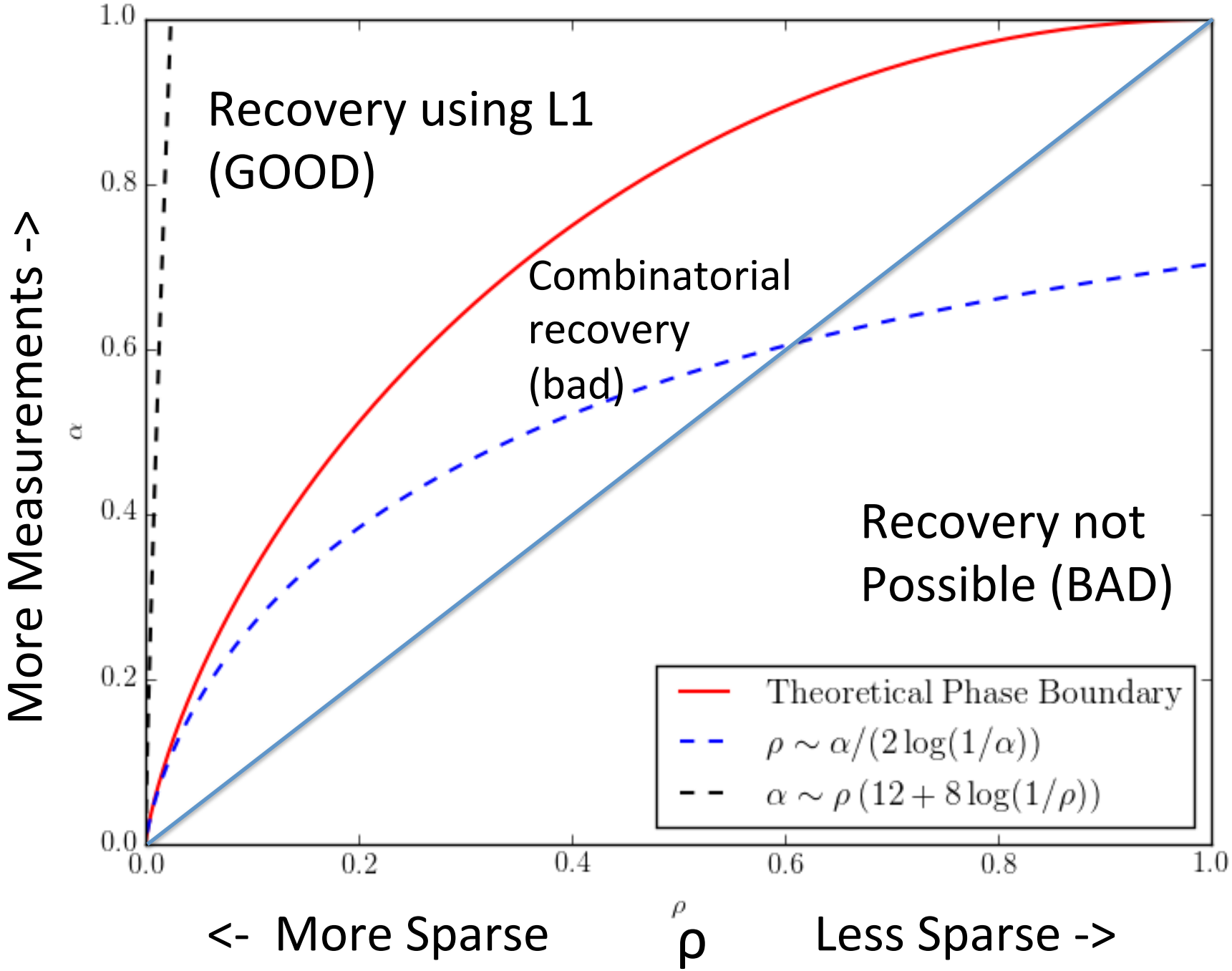
Recovery using L1
(GOOD)
Combinatorial
recovery
(bad)
Recovery not
Possible (BAD)
Theoretical Phase Boundary
$\rho \sim \alpha/(2\log(1/\alpha))$
$\alpha \sim \rho\,(12 + 8\log(1/\rho))$
More Measurements ->
<- More Sparse
ρ
Less Sparse ->
0.0
0.2
0.4
0.6
0.8
1.0

Other algorithms exist ...

What are the phase transition boundaries?
Universality classes?
Not well understood –> part of our motivation.

- L1 + L2 penalized regression (Elastic Net)
  - $X=\text{argmin}_x \, |Y-Hx|^2+ \lambda_1|x|+\lambda_2|x|^2$

- Iterative hard thresholding
  - $X_{n+1}=Th(X_n + H^*(y-Hx_n))$

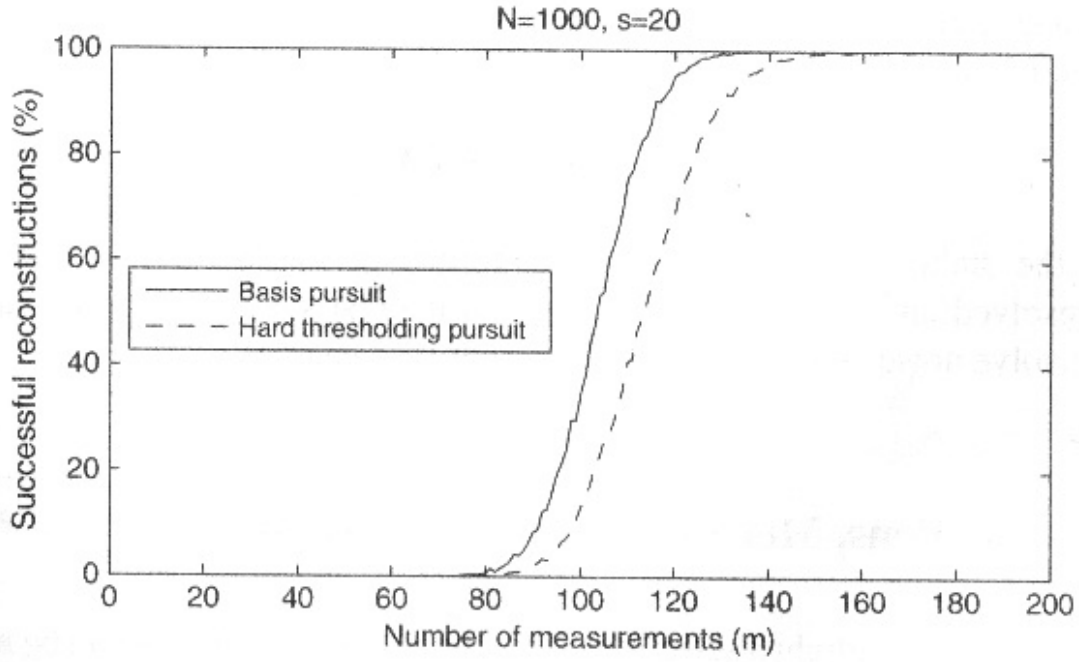

Algorithmic Phase Boundaries Differ: (have tradeoffs)

±1 sparse vectors (Basis pursuit better)

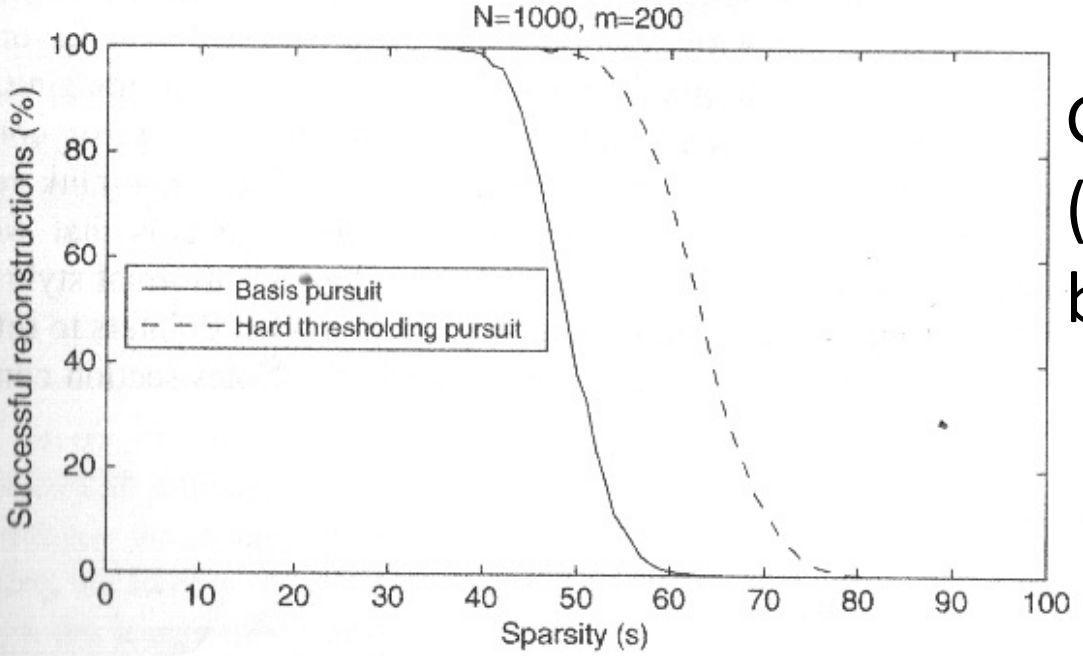

Gaussian sparse vectors (Hard-thresholding pursuit better)

Taken from "A Mathematical Introduction to Compressed Sensing" by Foucart and Rauhut P. 7

New Results

- New derivation of Mean Field Equations using Cavity method.
- Phase transition curve for Elastic Net (differs from Basis Pursuit curve)

- Non-trivial exponents obtained for Basis Pursuit
  - MSE(Basis Pursuit) ~ $\lambda^{4/3}$ On the phase transition line
  - MSE(Elastic Net) ~ λ (on the phase transition line)

- Basis Pursuit and Elastic Net exponents are different (existence of different universality classes)
- Exponents depend on behavior of probability distribution of parameters near origin.
- MSE shows minimum at non-zero λ for noise>0.

- Formulae for matrices with correlated entries.

Mean Field Equations:
Single Variable Optimization with
Stochastic Parameters + Self Consistency conditions

$$\hat{u}_a = \min_{u_a} \{ \frac{1}{2\sigma_{\text{eff}}^2} \left(u_a^2 - 2\xi_a u_a \right) + U(u_a + x_{0a}) \}$$

$$\xi_a \in \mathcal{N}(\xi; 0, \sigma_\xi^2) \text{ with } \sigma_\xi^2 \equiv \sigma_\zeta^2 + \frac{q}{\alpha}$$

$$q \equiv \sum_a [\hat{u}_a^2]_{x_0,\xi}^{\text{av}}$$

$$\sigma_{\text{eff}}^2 \equiv \sigma^2 + \frac{\overline{\chi}}{\alpha}$$

$$\overline{\chi} \equiv \frac{1}{N} \sum_a \chi^{aa}$$

Theory vs Simulations (Elastic Net)

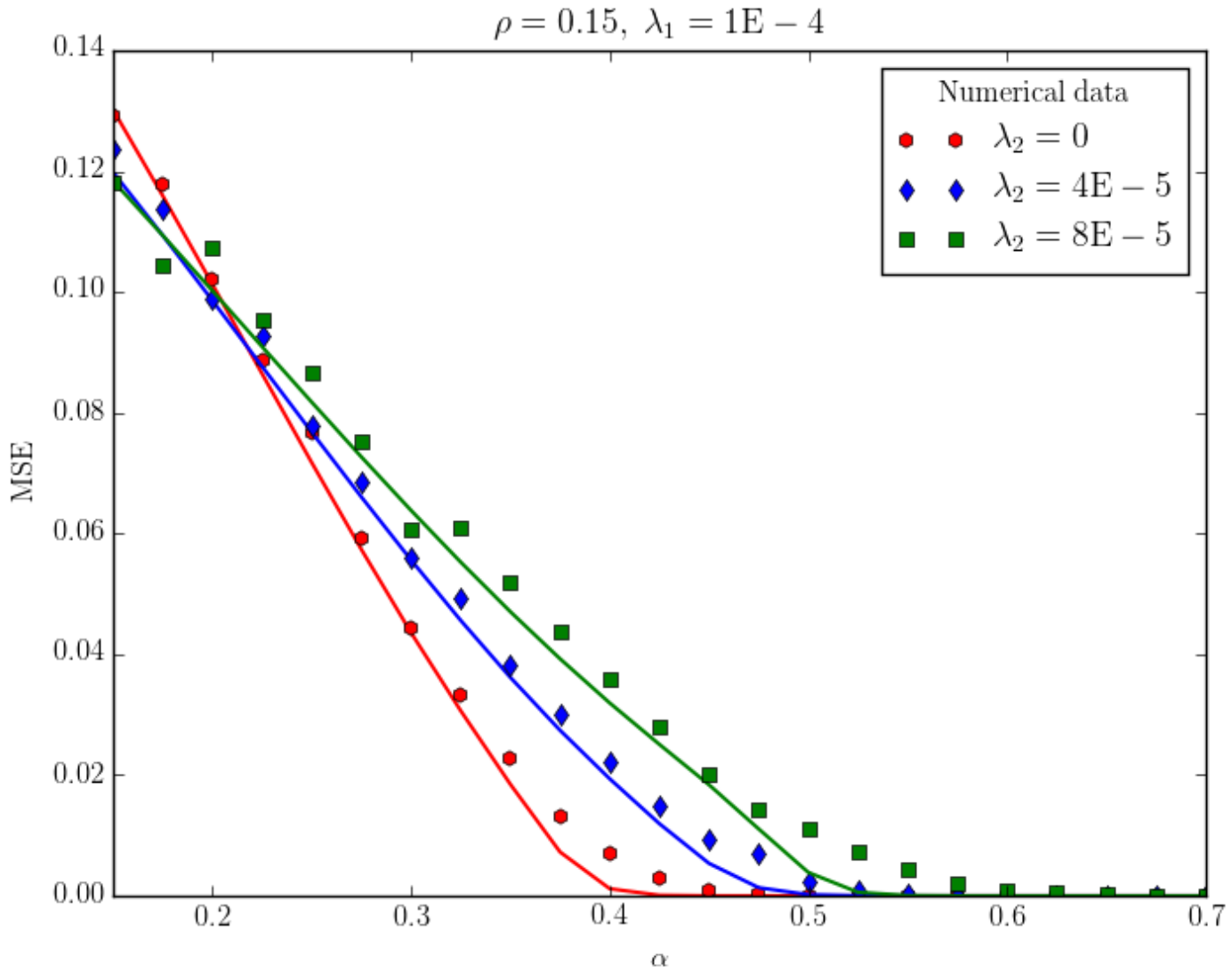

Mean Squared Error

More Measurements ->

For the finite noise case (Basis Pursuit),
MSE shows a minimum at $\lambda \sim (\text{Noise Variance})^{2/3}$
(Model selection criterion)

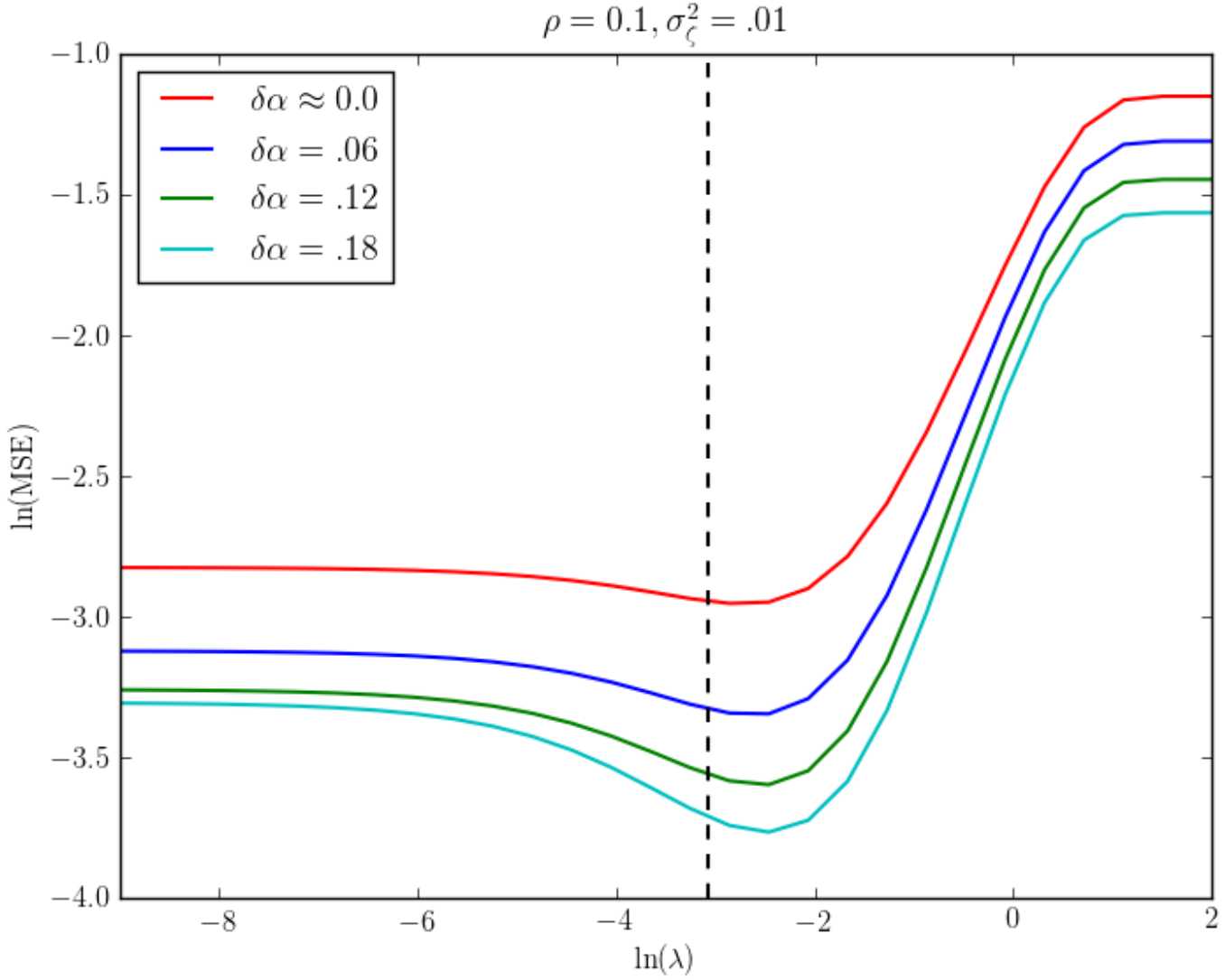

MBA Project Personnel

Research Staff

Ferenc Mechler *data analysis, reports*
Daniel Ferrante *data analysis, web programming*
Sotiris Raptis *data analysis, pipeline software*
Zvika Havkin *storage, system admin*

Laboratory Technicians

Alexander Tolpygo *Lab. management*
Stephen Savoia *tracer Injection, QC*
Kevin Weber *perfusion, IHC*
Neil Franciotti *cryosectioning*
Nicholas Baltera *cryosectioning*

RIKEN/CSHL

(Collaboration with Hideyuki Okano; Japan Brain Initiative)
Yeonsook Takahashi (Lab Manager)
Bingxing Huo (Data Analysis)
Adam Lin (Computation/sysadmin)
Kumkum Hassan (Lab Tech)

IIT Madras

Collaborating groups:

Sukhendu Das, Sutanu Chakraborty

Former Project Staff

Data Analysis

Swagatam Mukhopadhyay	*cell segmentation*
Amit Mukherjee	*image processing & analysis*
Pascal Grange	*injection grid plan*

Software

Osama El Demerdash	*LIMS, sysadmin*
Noah Jakimo	*software development, sysadmin*
Yingbing Zhang	*storage, sysadmin*

Project Pipeline

Vadim Pinskiy	*methods engineering, integration*
Caizhi Wu	*tracer injection*
David Pevzner	*cyrosectioning*
Jamie Jones	*cryosectioning*
Andrew Weber	*perfusion, immunohistochemistry*
Joshua Novy	*digital imaging*
Christin Bergano	*digital imaging*

Collaborators / Consultants

Marcello Rosa (Monash U, Australia)

Hideyuki Okano (RIKEN, Japan)

Stefan Geyer (MPI Leipzing)

Mihail Bota (UCSD)

Jason Bohland (BU)

Moritz Helmstaedter (MPI) & Lab

Josh Huang (CSHL) & Lab

Günter Giese (MPI Heidelberg)

Michael Hawrylycz (ABI)

Harvey Karten (UCSD)

Pavel Osten (CSHL)

Kathy Rockland (MIT)

Sebastian Seung (MIT)

Ian Wickersham (MIT)

Support

- Keck Foundation
- NIH (TR01 MH087988, RC1 MH088659, DA036400, MH105949, MH105971)
- Cold Spring Harbor Laboratory
- Crick-Clay Professorship
- Simons Foundation
- Mathers Foundation
- NSF INSPIRE and EAGER award
- Japan Brain Initiative (RIKEN)
- H. N. Mahabala Chair (IIT Madras)

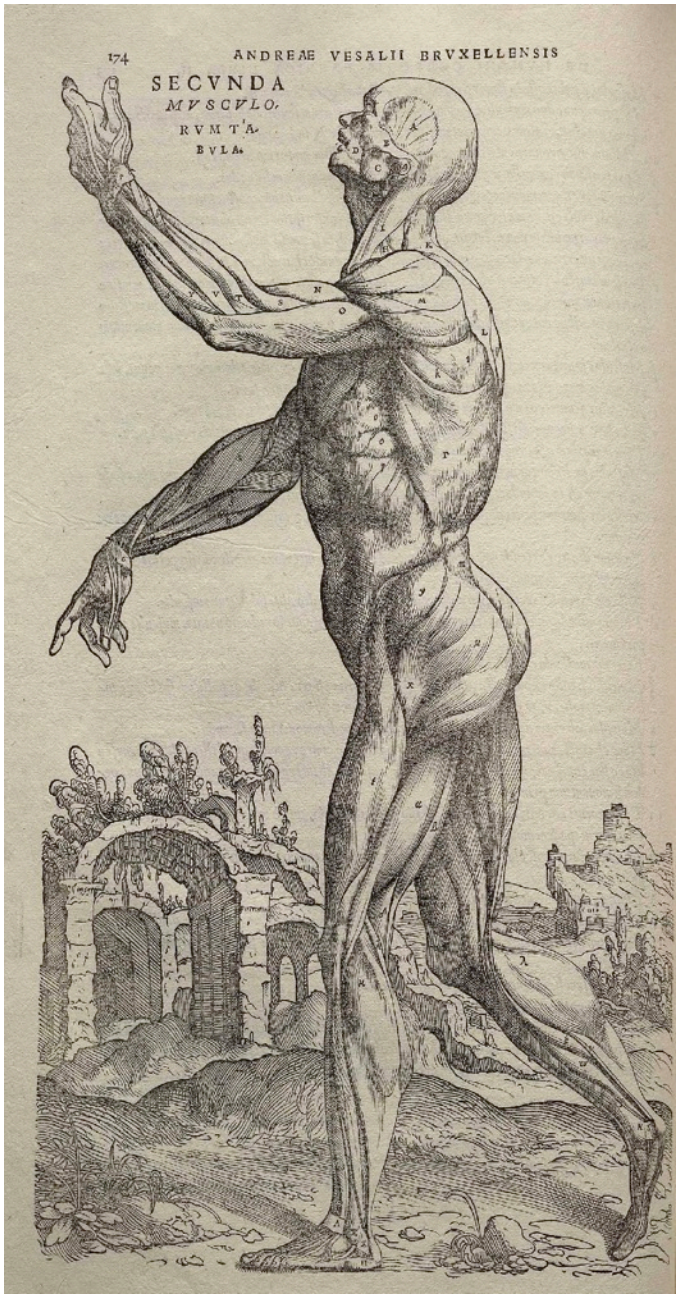
174 ANDREAE VESALII BRVXELLENSIS
SECVNDA
MVSCVLO.
RVMTA.
BVLA.